Thermo-optical performance of molecular solar thermal energy storage films

N.B. When citing this work, cite the original published paper.

(article starts on next page)

Thermo-optical performance of molecular solar thermal energy storage films

Zakariaa Refaa [a,*], Anna Hofmann [b], Marcial Fernandez Castro [c], Jessica O. Hernandez [b], Zhihang Wang [b], Helen Hölzel [b], Jens Wenzel Andreasen [c], Kasper Moth-Poulsen [b], Angela Sasic Kalagasidis [a]
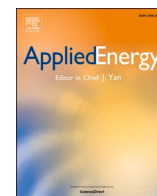
[a] Department of Architecture and Civil Engineering, Chalmers University of Technology, Gothenburg 412 96, Sweden
[b] Department of Chemistry and Chemical Engineering, Chalmers University of Technology, Gothenburg 412 96, Sweden
[c] Department of Energy Conversion and Storage, Technical University of Denmark, Fysikvej, 2800 Kgs. Lyngby, Denmark

HIGHLIGHTS

- Performance of MOlecular Solar Thermal energy storage (MOST) composite films for energy-saving windows.
- Transmission and energy storage of the MOST film can be controlled through molecular design and composite's formulation.
- Upon optimization, a 1 mm thick MOST film could store up to 0.37 kWh/m^2 and feature a heat release flux exceeding 4 W/m^2.

GRAPHICAL ABSTRACT
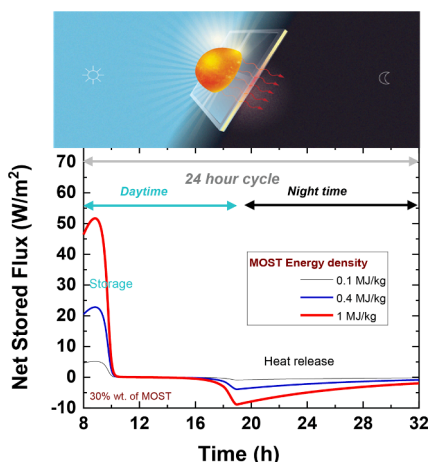
ARTICLE INFO

ABSTRACT

Due to their potential for solar energy harvesting and storage, molecular solar thermal energy storage (MOST) materials are receiving wide attention from both the research community and the public. MOST materials absorb photons and convert their energy to chemical energy, which is contained within the bonds of the MOST molecules. Depending on the molecular structure, these materials can store up to 1 MJ/kg, at ambient temperature and with storage times ranging from minutes to several years. This work is the first to thoroughly investigate the potential of MOST materials for the development of energy saving windows. To this end, the MOST molecules are integrated into thin, optically transparent films, which store solar energy during the daytime and release heat at a later point in time. A combined experimental and modeling approach is used to verify the system's basic

functionality and identify key parameters. Multi-physics modeling and simulation were conducted to evaluate the interaction of MOST films with light, both monochromatic and the entire solar spectrum, as well as the corresponding dynamic energy storage. The model was experimentally verified by studying the optical response of thin MOST films containing norbornadiene derivatives as a functional system. We found that the MOST films act as excellent UV shield and can store up to 0.37 kWh/m^2 for optimized MOST molecules. Further, this model allowed us to screen various material parameters and develop guidelines on how to optimize the performance of MOST window films.

Nomenclature

C_0	concentration of MOST (mol/m^3)
Abs	Absorbance (–)
C_p	specific heat capacity (kJ/(K•kg))
$\bar{E}_{300-460nm}$	average photon's energy in the wavelength range 300–460 nm (J)
$E_{storage}$	energy storage density (kJ/m^2)
G_λ	spectral solar irradiation (W/(m^2•nm))
$\Delta H_{storage}$	energy storage density of MOST (kJ/mol)
ΔH_{iso}	energy storage density in one QC molecule (J)
I	irradiation (W/m^2)
K	thermal conductivity (W/(K•m))
N_A	the Avogadro constant (1/mol)
NBD	concentration of norbornadiene (mol/m^3)
P	heat absorbed (W/m^3)
Q	heat release during back-conversion (W/m^3)
QC	concentration of quadricyclane (mol/m^3)
S	heat source (W/m^3)
T	temperature (K)
d	the film thickness and light pathway (m)
k	the rate constant for thermally induced isomerization (1/s)
$\dot{n}$	photon flux (photons/(s•m^2))
$t_{1/2}$	half-life time (h)
wt	weight (%)

Greek letters

α_λ	spectral absorption of PS film of thickness d (–)
β	absorbed fraction of light (–)
δ	degree of transformation of NBD
ε	molar absorptivity (1/(M•cm))
ϵ	emissivity (–)
η	efficiency (%)
λ	wavelength (nm)
ρ	density (kg/m^3),
σ	Stefan-Boltzmann constant (W/(m^2·K^4))
τ_λ	spectral transmission of PS film of thickness d (–)
ϕ or QY	quantum yield (–), (%)

Subscripts

BC	back-conversion
NBD	NBD molecules
Net	net flux
QC	QC molecules
PS_abs	polystyrene
$Stored$	stored flux
amb	ambient
$heat$	heat
$incident\_i$	incident irradiation entering the film
iso	isomerization
$storage$	stored energy
s	surface
$surr$	surrounding
$thermal\_iso$	thermally induced back-conversion

1. Introduction

Heating and cooling in buildings and industry account for half of the EU's energy consumption [1]. In EU households, heating and hot water alone account for 79% of total final energy use. To reduce the impact of heating on the environment, it is thus necessary to identify viable sources of renewable energy for heating and hot water supply, but also to make buildings more energy efficient. The earlier requires the development of efficient energy storage systems, which bridge the intermittency of renewable energy production. The latter can be addressed by improving the insulation of building, in particular of windows, which are responsible for a large share of all heat losses and heat gains in buildings [2,3].

Unlike traditional windows, smart windows can adjust their optical properties in response to solar irradiation and/or outdoor conditions, passively or actively. Thus, they have the potential to improve the energy efficiency of buildings and the indoor environment. Several solutions were developed to upgrade windows with new functions to increase the energy savings of buildings [4-6]. These solutions range from simple tinted glass to active dynamic coatings [6]. Among these solutions one can find low emissivity coatings and adaptable smart glazing such as thermochromic, photochromic,[5], and electrochromic glazing [3]. Several works attempted to evaluate the performance [4,6]

and the control strategies [7] of the new solutions for energy saving. In a recent study [4], three different solutions were compared for three different geographic locations. Electrochromic glazing showed the highest potential in lowering energy demand for all cases and locations. Further, the study highlights the importance of having the proper control strategy for the electrochromic windows to obtain the maximum effect [4,7].

Other novel solutions utilize energy storage materials such as phase change materials for the storage of thermal energy [8,9]. The incorporation of this function leads to an enhancement of thermal energy storage of the window and thus the decrease of thermal transmittance (U-value). However, the visible light transmittance decreases from 0.8 to 0.24 and 0.44 for liquid and solid phases, respectively, leading to poor light quality [8]. In comparison, MOlecular solar thermal energy STorage (MOST) materials [10-12] can offer a higher energy density than PCMs without influencing the visible transmittance of light. Unlike sensible and latent heat storage materials, which are charged with heat, the MOST molecules absorb solar irradiation, i.e., photons. Upon absorption of a photon, the MOST molecules undergo a chemical isomerization from a low (i.e., parent state, NBD) to a high-energy configuration (isomer state, QC) (cf. Fig. 1). In the isomer state, solar energy is stored in the chemical bonds of the molecules. When the molecules "switch back", to the low energy parent configuration, the stored energy (i.e. chemical energy) is released as heat. This charging and heat release cycle can be repeated thousands of times without
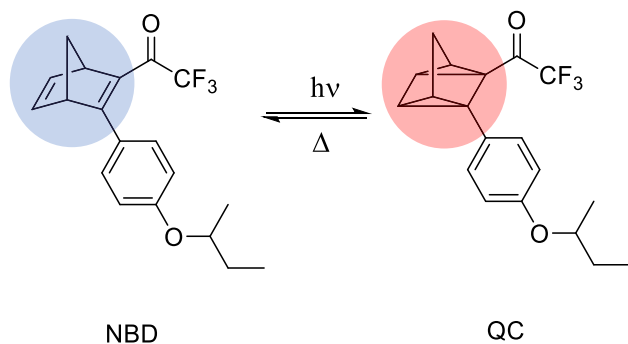
Fig. 1. Photoswitch molecule system for solar energy storage. The shaded circles highlight the Norbornadiene (NBD, parent state, blue) and Quadricyclane (QC, isomer state, pink) forms. (For interpretation of the references to color in this figure legend, the reader is referred to the web version of this article.)

significant degradation [13].

Depending on the exact molecular structure, the isomer state can be stable for different time spans at room temperature, which offers enormous potential for short-term and long-term renewable energy storage without substantial energy losses [10]. Currently available molecular photoswitches allow energy storage times ranging from parts of seconds to tens of years. The energy storage density of the MOST systems is higher than most latent heat energy storage systems, and can reach an energy density of up to 1 MJ/kg.[14]

A potential benefit of the MOST systems for applications is that the MOST molecules change their chemical state throughout charging and discharging cycles but not the phase (unlike PCM). Thus, the molecules retain their capacity to harvest and store energy when mixed into a solvent or polymer (solids). [13,15]. Furthermore, when MOST molecules can be used as additives in transparent polymers such as polystyrene, the visually clear appearance of the composite is unaffected by the switching process. This makes MOST-polymer composites attractive for applications that utilize the energy storage and heat release function, but that require at the same time high optical transparency.

One example for such applications could be windows with integrated transparent MOST composites which feature a thermal storage function for an improved energy management in buildings. This concept was discussed earlier by Miki and coworkers[13], and recently by Petersen et al. [15], who fabricated several MOST – polymer composites with high energy storage densities of up to 52 kJ/kg (for 11 wt% active compound) which showed minimal degradation over multiple cycles. However, these works, as well as most of the other available literature in the field, focuses on the absorbance properties of the film, whereas thermal aspects are not discussed. This is partly due to the fact that the energy storage and heat release in MOST systems are complex and dynamic, where the concentration of different isomers changes as a function of light exposure, temperature and time. Consequently, the study of such MOST composites requires an intricate multiphysics model that takes into account all of the underlying convoluted mechanisms in the material.

In the context of smart windows, the traditional performance criteria such as U-Value and Solar Heat Gain Coefficient (SHGC) [16] are not enough to describe the performance of a MOST film in a window since the dynamic energy storage is not accounted for in these figures of merit. Hence, a new performance indicator is needed to benchmark and communicate the performance of the new MOST solutions.

Thus, the model and performance indicators presented in this work aim to guide the future development of MOST molecules, towards systems whose properties are optimized for the use in smart windows.

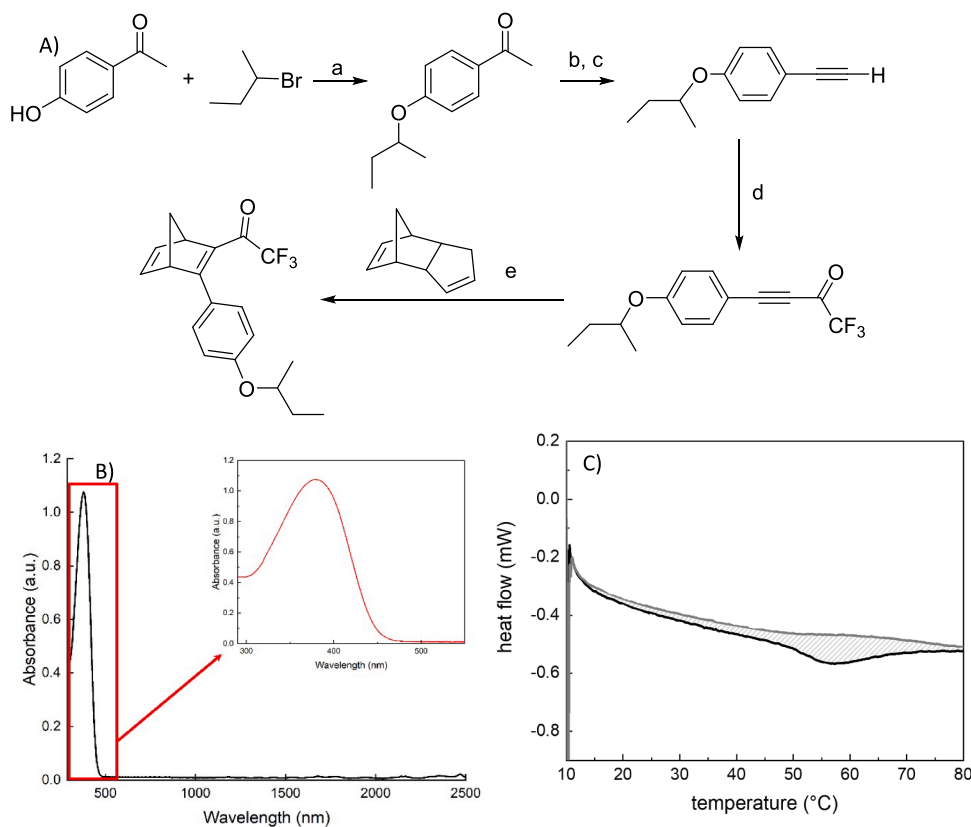Our goal is to study the performance of the MOST coatings for energy

Fig. 2. A) Synthesis pathway for NBD molecules, B) UV/Vis absorption spectrum of the NBD and QC molecule in toluene, and C) DSC scan of an NBD – polystyrene composite with 10 wt% NBD (black line = first heating, gray line = second heating) with the highlighted area corresponding to the stored energy.
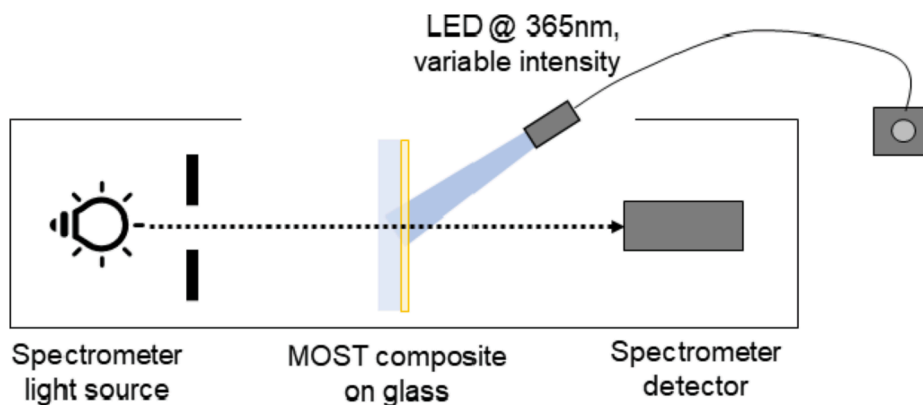
Fig. 3. Scheme of the experimental illumination setup.

savings and provide a detailed model that describes the physical effects of these coatings upon exposure to sunlight. Besides describing and quantifying relevant thermochemical processes occurring in the composite under realistic operation conditions, new performance indicators are proposed. The latter aims to quantify the basic performances of the composite (e.g. energy storage, efficiency, and storage time) and, thereby, to guide future research on MOST systems. To study the MOST film composite interaction with solar irradiation in detail, a numerical model has been developed in COMSOL Multiphysics®. The equation describing the rate at which chemical species form/decay and the heat balance equation were coupled to simulate the thermo-optical performance of a polystyrene/MOST composite film. The model allows dynamic simulations of the thermal and optical response of the composite for different molecules and under various irradiation conditions. In addition, the effects of MOST molecular characteristics such as the molar absorptivity, the quantum yield of the absorption and storage process, the energy storage density, as well as the storage time have been studied. Finally, the MOST film energy storage and optical behaviors are simulated for monochromatic light as well as full spectrum solar irradiation.

Furthermore, a newly designed Norbornadiene (NBD)/Quadricyclane (QC) molecular system embedded in a polystyrene matrix is used as a proof of principle demonstration. The system initially exists in low energy and orange-yellow NBD form that, upon irradiation, is converted to the high energy and colorless QC isomer form (Fig. 1). The theoretical models of photoisomerization and back-conversion of MOST molecules in the polystyrene film were validated by comparing the simulated data to experimental data from composites films with various thicknesses and concentrations.

2. Materials and methods

The photoswitching molecule used for this study is based on a norbornadiene (NBD) which is substituted with a trifluoroacetyl acceptor group and an aromatic donor group bearing an isopropyl side chain. The molecule was obtained following a five steps synthesis pathway, as illustrated in Fig. 2.

The molecular photo-switch NBD absorbs sunlight (<460 nm), resulting in the formation of a high-energy isomer QC. Over time, the metastable QC isomer relax back to the parent NBD form, releasing the stored energy ($\Delta H_{storage}$ (kJ/mol)) as heat. This process is a thermally activated unimolecular reaction and can thus be described by an exponential decay function, also known as the Eyring or Arrhenius equations. The half-life time of the back-conversion is often referred to as storage half-life time ($t_{1/2}$) of the high-energy isomer.

The optical properties of the NBD/QC system (see Fig. 2b), as well as the kinetics of the back-conversion from QC to NBD were measured in solution. To this end, the NBD compound was dissolved in toluene at a concentration of <0.1 mM and transferred into a quartz cuvette with a 1

cm pathlength. All UV/Vis absorption spectra were measured using a Cary 60 UV/Vis spectrometer. The photoconversion from NBD to QC was performed using a LED at 365 nm from Thorlabs (M365F1). The back-conversion from QC to NBD over time at room temperature was followed by UV/Vis spectrometry (see Fig. 3), and the maximum absorption was traced as a function of time.

The quantum yield (QY) of the photoconversion process in alkylated NBD derivatives of the same family as the one that was used in this work were measured by actionometry, following the published procedure using potassium ferrioxalate and tris-phenanthroline iron (II) complex [15,17]. The QY of NBD/QC in toluene was found to be 51.4 ± 0.5%. Recently it has been shown that the QY of NBD molecules of this family within plastic composites can even exceed their QY in solution [17]. For simplification, we thus assumed a QY of 51.4 % for our calculations since a detailed analysis of the QY was outside the scope of this work.

The energy storage density of the NBD/QC system was measured on NBD – polystyrene composite samples. To this end, polystyrene PS (purchased from Sigma Aldrich with a molecular weight M_w of 192 000 g/mol) was dissolved in toluene (c = 200 g/l) under magnetic stirring for 12 h at room temperature. Then, the NBD molecule was added to the polystyrene solution to yield a solution containing 10 wt% NBD with respect to the polystyrene content. The solution was drop cast on a glass slide and dried in the dark at room temperature overnight under ambient conditions. The sample was placed under a solar simulator (EYE Solarlux 150 W) and illuminated for 3 h in order to photoconvert the NBD molecules in the sample into their QC form. At least 5 mg of the composite material were then placed in a Mettler Toledo differential scanning calorimetry (DSC) aluminum pan. The energy storage density of the composite was then measured with the DSC (heating rate 3 K/min) by comparing the first heating cycle to the second heating cycle (see Fig. 2c). The 10 wt% MOST composite showed an energy storage density of ΔH = 0.01 MJ/kg and the NBD molecule of ΔH = 0.1 MJ/kg ($\Delta H_{storage}$ = 34 kJ/mol, calculated as /M_w), respectively. We note that the measured energy density of this particular molecule is lower than the reported value for other NBD/QC systems [14], which we attribute to the incomplete charging due to the optical overlap between QC and NBD states of the molecule (Fig. 2b).

2.1. Preparation of composite films

For the preparation of the composite films, polystyrene was dissolved in toluene under magnetic stirring, as stated previously. Then, the NBD molecules were added to the polystyrene solution to yield a solution containing either 0.5 wt% or 5 wt% of NBD molecules with respect to the polystyrene content. The solution containing 0.5 wt% NBD, was drop cast on a glass slide and dried in the dark at room temperature under ambient conditions for at least 3 h, yielding films with a thickness of 57 ± 3 μm, 45 ± 2.2 μm, and 61 ± 3 μm. The film thickness was determined

Table 1
Summary of the film composite characteristics.

MOST molecule	
Molar absorptivity @ 365 nm (1/(M•cm))	QC: 251.5
	NBD: 7410
Molecular weight (g/mol)	336.3
The energy density (kJ/mol)	34
Quantum yield (%)	51.4 ± 0.50
Polystyrene and MOST molecules	
Density (kg/m^3)	1030
Thermal conductivity (W/(m·K))	0.14
Heat capacity (J/(kg·K))	1400
Emissivity ϵ	0.9

with a caliper. The solution containing 5 wt% of NBD, with respect to the polystyrene, was spin-cast onto glass slides, yielding films with a thickness of 4.1 ± 0.2 μm, 2.6 ± 0.1 μm, and 4.7 ± 0.2 μm. The thickness of the spin-cast films was measured with a profilometer. The concentration of NBD in the dry composite was 0.5 wt% (15.3 mol/m^3) and 5 wt% (153.11 mol/m^3).

2.2. Light exposure and recovery of thin composite films

The optical properties of the NBD/QC molecules in toluene solution and of the composite films were measured using a Cary 60 UV/Vis spectrometer (Agilent). The maximum absorption was located at 382 nm. The molar absorptivities of the QC and NBD form at 382 nm, measured in toluene solution, were 236 1/(M•cm) and 8005 1/(M•cm), respectively. The composite was converted from its NBD to QC form using a Thorlabs LED (365 nm) with an irradiation power of 120 mW, which corresponded to a photon flux of $8.8 \cdot 10^{14}$ 1/(cm^2•s).

The film was illuminated with the LED from ca. 3 cm distance, and the exposed spot on the composite films was ca. 1 cm^2. During the exposure and photoconversion process (NBD to QC), the absorption spectrum of the composite was monitored at a measurement interval of 12 s. After illumination, film was left to recover (QC to NBD) in the dark at ca. 25 °C, while the absorption spectrum was monitored over time. In Table 1 we summarize the properties of the MOST molecule and of the composite film.

3. Energy and optical modeling

3.1. MOST film system definition

The MOST composite film is modeled as a multicomponent domain consisting of the MOST molecules dispersed in a polymer matrix (e.g., polystyrene). Then, a monochromatic or polychromatic light source is directed at an angle of 90° to the film's surface plan, which is also the main direction for heat and light transfer analysis.

The molar concentration of the MOST molecules in the film is constant and equal to C_0 [mol/m^3]. Depending on the illumination and the state of isomerization, the MOST molecules in the film may exist as both NBD and QC isomers. The instantaneous molar concentrations of these isomers satisfy the molar balance equation:

$$[NBD] + [QC] = C_0 \tag{1}$$

Note that both $[NBD]$ and $[QC]$ are time-dependent, but the time parameter is omitted in their notations for simplicity reasons. The conversion rates between the two isomers are described in the following section (cf. Photoisomerization reaction). The total number of the MOST molecules per 1 m^2 of the film is also of interest

$$N_A \bullet d \bullet C_0 \tag{2}$$

where d is the thickness of the film (also the length of the light's pathway), and N_A is the Avogadro constant.

In the following sections, we provide the models behind the NBD

molecules' photoisomerization rate, energy balance, and boundary conditions. The light interaction with the MOST composite film is modeled in two steps: first, the model is derived for the monochromatic irradiation and then generalized for solar irradiation.

3.2. Monochromatic irradiation of the MOST composite film

3.2.1. Photoisomerization reaction

NBD's photoisomerization rate is modeled for a general case, where both NBD and QC absorb light. The photoisomerization is possible only from NBD to QC, whereas QC absorbs photons only to convert them into thermal energy. The concentration of QC during photoisomerization increases at the same rate as the concentration of NBD decreases. Some QC molecules convert back to NBD during the photoisomerization due to the thermally induced isomerization from QC to NBD (i.e. back-conversion). These molecules are denoted $[QC]_{BC}$. Hence, NBD's resulting conversion rate is found as a sum of the photoisomerization and the back-conversion contributions.

Before giving the expression of the NBD's photoisomerization equation, we define some relevant physical properties. Firstly, the total absorbance of the MOST molecules in the film, $Abs(t)$, is described following the Beer-Lambert law [18] for the case of several absorbing molecules [19]:

$$Abs(t) = ([NBD] \bullet \varepsilon_{NBD} + [QC] \bullet \varepsilon_{QC}) \bullet d \tag{3}$$

where ε_{NBD} and ε_{QC} are the molar absorptivities (1/(M•cm)) of the NBD and QC isomers at a given wavelength.

The absorbance is a function of time as each molecule's concentration depends on time and photon flux. In the photoisomerization wavelength range of the current MOST molecules [300 nm, 460 nm], the absorption of light by the polystyrene film can be neglected (the 1 mm thick polystyrene film absorbs about 0.9% of solar irradiation cf. Appendix 1). Thus, the total absorbed fraction of light by the MOST composite film is due *only to the MOST molecules* and can be calculated as follow [19,20]:

$$\beta(t) = \left(1 - 10^{-Abs(t)}\right) \tag{4}$$

The total absorbed light by MOST molecules is the sum of the absorbed fraction of light by NBD and QC molecules [19,20]:

$$\beta = \beta_{NBD} + \beta_{QC} \tag{5}$$

β_{NBD} and β_{QC} can be found by weighting the absorbance of NBD and QC with the total absorbance of the MOST system [20]. The fraction of light absorbed by NBD and QC molecules is [19,20]:

$$\beta_{NBD} = \frac{[NBD] \bullet \varepsilon_{NBD} \bullet d}{Abs} \left(1 - 10^{-Abs}\right) \tag{6}$$

$$\beta_{QC} = \frac{[QC] \bullet \varepsilon_{QC} \bullet d}{Abs} \left(1 - 10^{-Abs}\right) \tag{7}$$

Finally, the change in NBD concentration is given by the following equation:

$$\frac{d[NBD]}{dt} = -\frac{\phi_{NBD} \bullet \dot{n} \bullet \beta_{NBD}(t)}{N_A \bullet d} - \frac{d[QC]_{decayed}}{dt} \tag{8}$$

$\dot{n}$: photon flux photons/(s•m^2)
ϕ is the photoisomerization quantum yield, which is defined as the number of converted molecules per absorbed photon.

The first part of the equation's right-side accounts for the photoisomerization caused by irradiation. In contrast, the second part is the
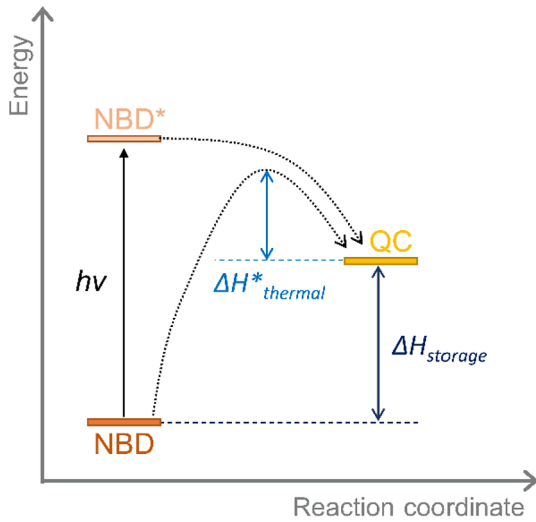
Fig. 4. Energy state versus reaction coordinate.

back-conversion mechanism. A first-order reaction is usually adopted to describe the back-conversion of QC as a function of time [20]. The rate of back-conversion of QC in this case:[1]

$$\frac{d[QC]_{BC}}{dt} = \frac{\partial [QC]}{\partial t} = -k[QC] \tag{9}$$

where k is the rate constant for thermally induced isomerization (1/s). The rate of back-conversion of QC molecules is proportional to the molar concentration of QC at time t.

Finally, the conversion rate of NBD during the photoisomerization can be found by solving the following ordinary differential equation [20]:

$$\frac{d[NBD]}{dt} = -\frac{\phi \bullet \dot{n} \bullet \beta_{NBD}}{N_A \bullet d} + k[QC] \tag{10}$$

3.2.2. MOST molecules induced heat source

The photoisomerization and thermal isomerization processes influence the energy balance of the MOST composite film. The absorbed fraction of the incident light by NBD molecules is:

$$I_{incident\_in} \bullet \beta_{NBD} \tag{11}$$

where $I_{incident\_in}$ is the incident monochromatic irradiation (W/m^2), that enters the film.

The photon energy absorbed by the molecules during the photo-isomerization of NBD can be expressed as the sum of the energy stored as chemical energy and the gain in thermal energy. The thermal energy gain can be ascribed either to vibrational relaxation of the excited state NBD* back to the NBD ground state (i.e. the photoisomerization quantum yield $\phi < 1$) or to the vibrational relaxation into the metastable state of the quadricyclane (cf. Fig. 4) [21].

First, the storage capacity of a single molecule is calculated from $\Delta H_{storage}$ (kJ/mol):

$$\Delta H_{iso} = \frac{\Delta H_{storage}}{N_A} \tag{12}$$

We define $I_{storage}$ (W/m^2) which describes the rate at which chemical energy is stored in NBD molecules:

$$I_{storage} = [\phi \bullet \dot{n} \bullet \Delta H_{iso}] \bullet \beta_{NBD} \tag{13}$$

The heat flux absorbed by the NBD isomers can be then expressed as the difference between the total incident irradiation and the part that is chemically stored

$$I_{heat\_NBD} = [-\phi \bullet \dot{n} \bullet \Delta H_{iso} + I_{incident\_in}] \bullet \beta_{NBD} \tag{14}$$

Then, the volumetric heat source P_{NBD} (W/m^3) is found as

$$P_{NBD} = \frac{I_{heat}}{d} = \left[\frac{-\phi \bullet \dot{n} \bullet \Delta H_{iso} + I_{incident\_in}}{d}\right] \bullet \beta_{NBD} \tag{15}$$

Similarly, the absorbed light by QC molecules as heat (W/m^3) is written as

$$P_{QC} = \left[\frac{I_{incident\_in}}{d}\right] \bullet \beta_{QC} \tag{16}$$

3.2.3. Heat release kinetics

The chemical energy that is stored in the composite film, i.e., within the QC molecules, is then released as heat during the back conversion of QC to NBD. The stored chemical energy in a QC molecule is $\Delta H_{storage}$ (e.g. Eq. (12)), which correspond to the potential energy difference between QC and NBD molecule (cf. Fig. 4).

The heat release (W/m^3) due to back conversion is given in the following form:

$$Q_{thermal\_iso} = -\frac{d[QC]_{BC}}{dt} \bullet \Delta H_{storage} \tag{17}$$

Thus,

$$Q_{thermal\_iso} = k \bullet [QC] \bullet \Delta H_{storage} \tag{18}$$

The maximum heat release is proportional to the highest concentration of QC in the MOST film $[QC] = C_0$.

3.3. Generalization: interaction of solar irradiation and the MOST film

- The considered solar spectrum [300 nm, 2500 nm] will be divided into two wavelength intervals. The first one is [300 nm, 460 nm], where the photoisomerization of NBD occurs, and the second interval includes the rest of the solar spectrum [460 nm, 2500 nm]. We assume in the following that: In the wavelength [300 nm, 460 nm], that all the photons:
  - o have the same probability of inducing the isomerization of NBD (in accordance with Kasha's rule).
  - o possess the same average value of photon energy $\bar{E}_{300-460nm}$ (calculated as the total irradiation in [300 nm, 460 nm] divided by the photon flux in this wavelength interval).
- Because the focus of the work was on modeling the interactions between the light and the MOST film, the reflection of light on the film surface is omitted. In reality, the reflected part on the window glazing is about 8 % of the total solar irradiation [22], which is much lower than the transmitted part. Although we slightly overestimate the intensity of the transmitted light, the findings are still valid.
- MOST molecules do not absorb photons in the interval [460 nm, 2500 nm]. The PS is transparent for the photons in the range where MOST is photoactivated (300 nm and 460 nm). However, it absorbs photons outside this range. The absorbed fraction of solar irradiation solely by the polystyrene film is calculated as follows:

$$I_{PS-abs} = \int_{460}^{2500} \alpha_\lambda G_\lambda d\lambda \tag{19}$$

G_λ (W/(m^2•nm^1)) is the spectral solar irradiation which enters the MOST film, (cf. Fig. 5), similar to the monochromatic incident light defined earlier $I_{incident\_in}$.

α_λ is the spectral absorption of PS film of thickness d and deduced from the absorbance curve of PS film (Cf. Appendix 1) using Beer-Lambert law [19].

---

[1] the derivative of QC is partial, since the total change in the concentration of [QC] depend on the decay process and the photoisomerization.
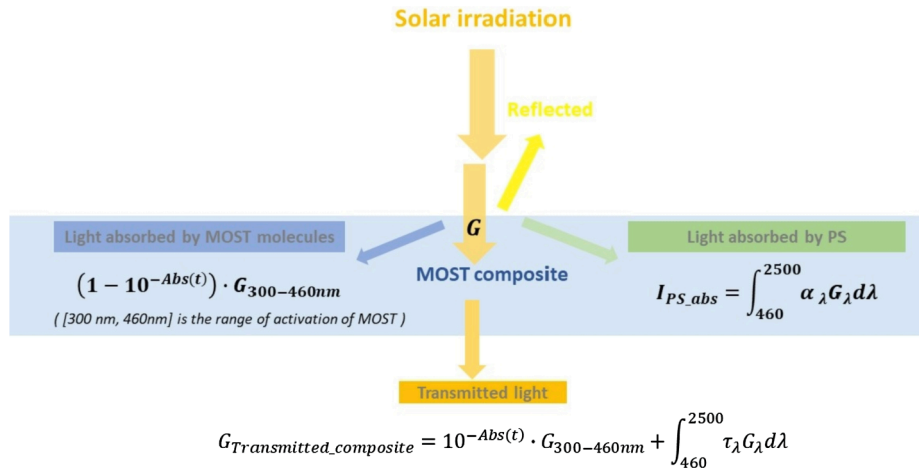
Fig. 5. Absorbed and transmitted solar irradiation by MOST film.

Thus, the absorbed solar irradiation by the MOST film is the sum of the absorbed fraction of light by NBD/QC molecules in the photoisomerization range [300, 460 nm] and the matrix of PS in the range [460, 2500 nm] (cf. Fig. 5). The absorbed solar irradiation by the composite reads

$$G_{absorbed_{composite}} = \left(1 - 10^{-Abs}\right) \bullet G_{300-460nm} + I_{PS_{abs}} \qquad (20)$$

where $G_{300-460nm} = \int_{300}^{460} G_\lambda d\lambda$.

The first term in the right-hand of equation Eq. (20) includes the energy stored and absorbed as heat in the MOST molecules, as shown in the previous section. And P_{PS_abs} (i.e., $\frac{I_{PS\_abs}}{d}$) is accounted for as a heat source term in the MOST film, as shown in Eq. (21).

Thus, the source term S in the MOST film is the sum of the following contributions:

$$S = P_{NBD} + P_{QC} + Q_{thermal\_iso} + P_{PS\_abs} \qquad (21)$$

For wavlengths between 300 nm and 460 nm, the heat gain resulting from the absorption of light by polystyrene matrix can be neglected because the PS matrix is almost transparent (0.9% absorbed with 1 mm thick film cf. Appendix 1). If the entire solar irradiation spectrum is considered, the matrix's absorption is significant and a heat gain term P_{heat_PS} should be included in the energy balance.

Following the same logic, the light transmitted by the MOST film is expressed as (cf. Fig. 5):

$$G_{Transmitted\_composite} = 10^{-Abs} \bullet G_{300-460nm} + \int_{460}^{2500} \tau_\lambda G_\lambda d\lambda \qquad (22)$$

3.4. Energy balance of the MOST film

Heat transfer through thin films and coatings for window applications is generally a three-dimensional (3D) problem. Taking into account that the thickness of a film is many times smaller than its width and length, it is commonly assumed that the 3D thermal effects are localized to the parts close to the frame. In the central parts of the film, which are considered in this work, the heat transfer is treated as one-dimensional.

For the purpose of numerical modeling, the MOST film domain is designed as 2D geometry, for which the following heat balance equation for the MOST composite film applies.

$$\rho C_p \frac{dT}{dt} = K \bullet \left(\frac{\partial^2 T}{\partial x^2} + \frac{\partial^2 T}{\partial y^2} \right) + S \qquad (23)$$

where T, ρ, C_p and K are the temperature (K), density (kg/m^3), specific heat capacity (kJ/(K•kg)), and thermal conductivity (W/(m•K)) of the

MOST film. All properties of the film contained in Eq. (23) are assumed to be constant. The heat source term in Eq. (23), is the combination of different processes: photons absorbed by NBD, QC, and polystyrene film, according to Eq. (21).

Geometry, boundary conditions, and initial values are defined as follows:

- The film dimension is 1 m × 0.001 m (length × thickness)
- The solar irradiation G interacts with the MOST film through absorption (chemical and thermal), and transmission, as shown in Fig. 5.
- To keep the focus on thermal processes resulting solely from the interaction between the solar radiation and the film, the ambient temperature T_{amb} is the same on both sides of the film and constant (20 °C); for the same reason, the initial temperature of the film is set to 20 °C.
- Neumann boundary conditions are prescribed to model the convective heat exchange between the long sides of the film and the ambient, $n \bullet q = h(T_s - T_{amb})$, where $n \bullet q$ denotes the heat flux in normal direction to the film surface. T_s is the temperature of the film surface that is calculated at each time step. For symmetry reasons, the convective surface heat transfer coefficient $h = 6$ W/(m^2•K) is the same and constant on both sides of the film; the chosen value represents an average of indoor and outdoor convective surface transfer coefficients typically found in buildings [23].
- Infrared radiation exchange between the film and the surrounding is described by the Stefan-Boltzmann Law: $n \bullet q = \sigma \epsilon (T_s^4 - T_{surr}^4)$, where T_s and T_{surr} are the temperature of the film surface and of the surrounding in (K). The temperature of the surrounding equals the ambient temperature $T_{surr} = 293.15$ K; the emissivity of the film is ϵ, and $\sigma = 5.67 \bullet 10^{-8}$ W/(m^2 K^4) is the Stefan-Boltzmann constant.
- Short edges of the film are defined as adiabatic surfaces, $n \bullet q = 0$.

3.5. Numerical solver

The equations were programmed in COMSOL Multiphysics 5.5, which is FEM-based software. Concerning the solving method approach, we used the following modules:

- The heat transfer module: to solve the energy balance equations in the film and the glass and to account for thermal boundary conditions
- The non-linear photoisomerization equation Eq. (10) and integral formulas are solved using the ordinary differential equation (ODE) from the equation-based modeling module (Mathematics module)
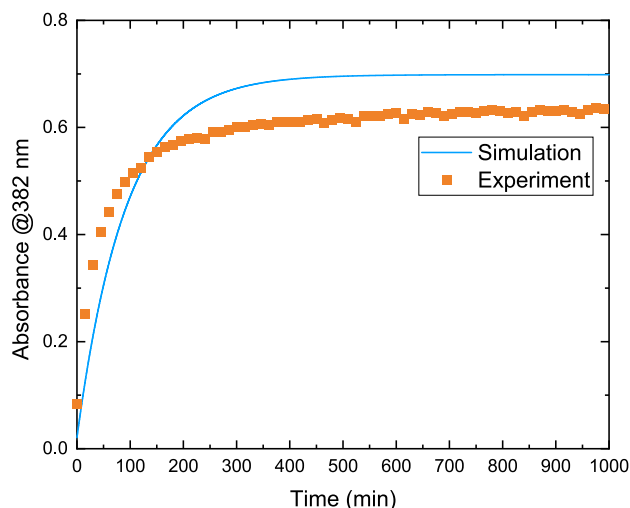
Fig. 6. Absorbance of the MOST film composite during illumination for a) thick films with 0.5 wt% and b) thin films with 5 wt%.

An adaptative time step with the relative tolerance of 10^{-6} and a physics-controlled mesh with fine mesh element size were used in all simulations.

4. Results: validation of photoisomerization rate equation

The absorbance of the MOST film was monitored over time during illumination with an LED (365 nm) and recovery in the dark. The absorbance decreases with irradiation time, as shown in Fig. 6. It levels off at an absorbance value of less than 0.1. The decrease in the absorbance of MOST films during illumination results from the photo-isomerization of NBD molecules, which are highly absorbing, into QC molecules, which show a much lower molar absorptivity.

The experimental and simulation results of the films' absorbance during illumination are shown in Fig. 6.

The model predicts the evolution of the absorbance of thick and thin films for different concentrations due to photoisomerization (cf. Fig. 6). The decrease of absorbance versus time and the saturation behavior are described by the model with appropriate accuracy. The back-conversion mechanism of QC to NBD was modeled using a first order exponential decay.

After complete conversion from NBD to QC, the recovery experiment

took place in the dark at 25 °C. During the recovery phase, the absorbance increases with time since QC molecules convert to the NBD form; however, it does not reach the initial absorbance value of the film composite (cf. Fig. 7).

Fitting with an exponential decay function yielded a back-conversion constant of $k = 1.8 \; 10^{-4} \; 1/s$ and a half-life time $t_{1/2}$ of almost 1 h at 25 °C. The absorbance shows a different relaxation path from the first-order decay mechanism [20], as shown in Fig. 7.

As mentioned in previous work, we assume that the local environment around QC molecules may influence the kinetics of the back conversion [24]. In the case of the composite discussed here, the MOST molecules are surrounded by a polystyrene matrix which is in a glassy state at the ambient temperature. This means that the mobility and flexibility of the PS chains is limited, which in turn may affect the isomerization kinetics of the embedded NBD/QC molecules. However, the exact mechanism of the back conversion in the polymeric matrix is not understood yet and will be the subject of upcoming work.

For simplicity reasons we used a first-order decay model to describe the photoisomerization and back-conversion kinetics for all of the following models presented in this work. We assume that this simplification provides sufficient accuracy for a meaningful simulation of the MOST composite characteristics (molecular and composite properties) and their influence on the thermo-optical properties of the MOST film.

In contrast to this validation experiment, where a narrow band LED was used to illuminate the composite, a MOST film in a window under real conditions will interact with the entire spectrum of solar irradiation. Thus, the performance of the MOST film should be studied in the whole wavelength range of photoisomerization of NBD molecules, which is [300 nm, 460 nm] for the studied MOST molecule.

5. Results: parametric study of the MOST film

5.1. Parametric study

The MOST molecules possess several parameters that can be engineered during the design of new MOST systems. To identify potential applications of MOST molecules, it is necessary to quantify the impact of the different molecular parameters on the energy storage and optical performance of the MOST film. In the following, the performance of the film is studied for different sets of molecular and composite parameters. The study aims to approach real solar irradiation. The NBD/QC system is active only in the wavelength range from 300 nm to 460 nm (cf. Fig. 2). In this range, we consider an average molar absorptivity $\overline{\varepsilon}_i$ for NBD and QC defined as
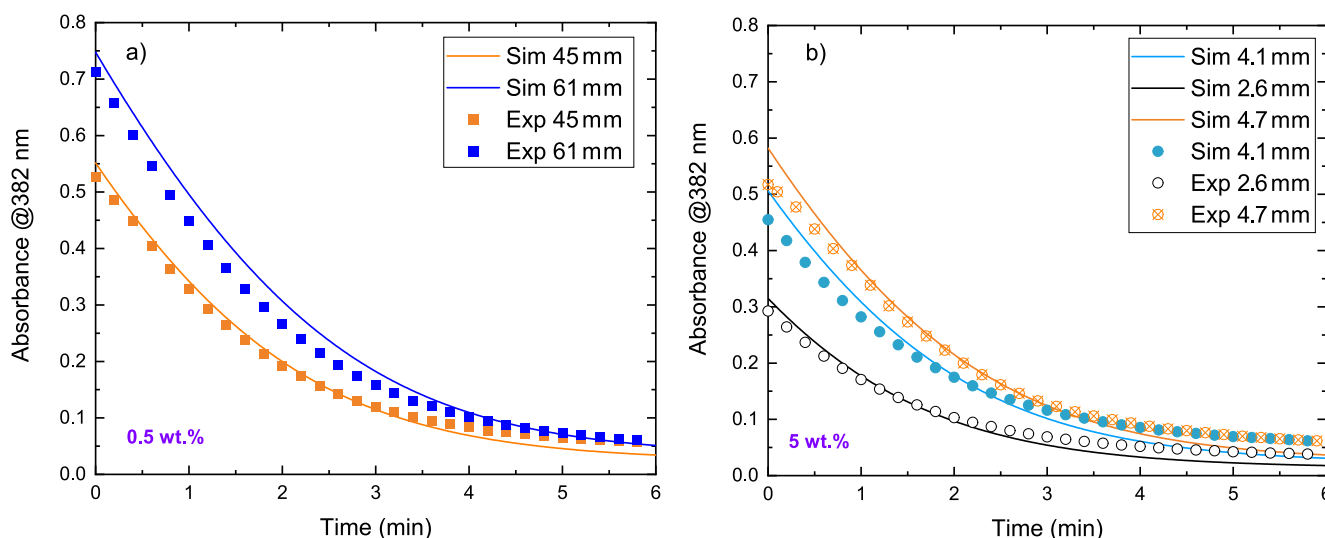

Fig. 7. Absorbance of MOST film during the recovery phase in the dark (0.5 wt% and 57 μm thick film).
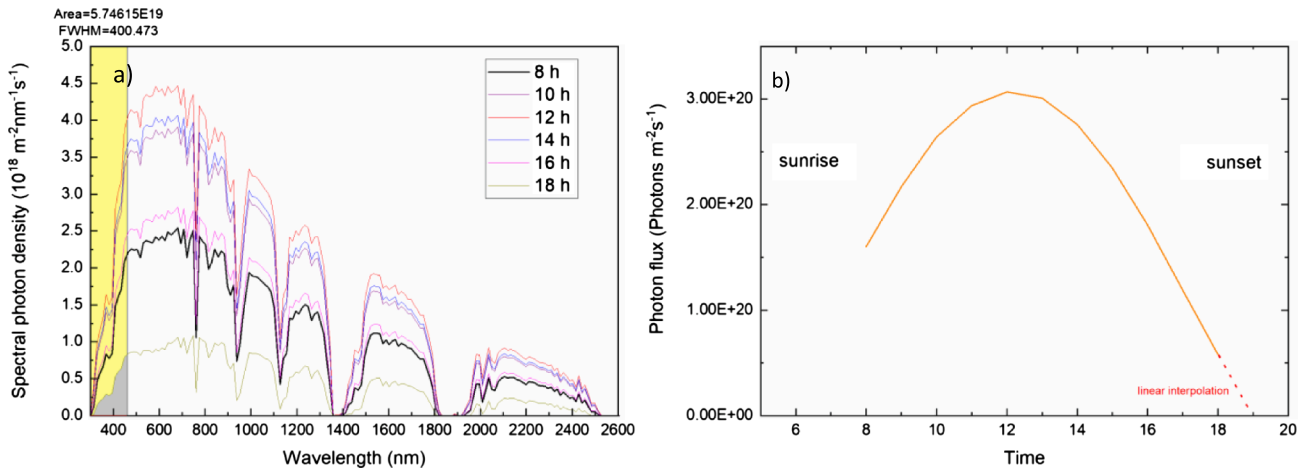
Fig. 8. Hourly spectral photon flux at different times a) at all wavelengths b) in the wavelength range [300 nm 460 nm].

Table 2
Case studies.

Case studies	Studied Parameters
Case 1	MOST concentration wt. % in the film
	0.5%, 5% 15% 30% 50% 70% and 90%
• 1 mm thickness	
• $\overline{\varepsilon}_{NBD}$ = 4590.8 1/(M•cm) and	
$\overline{\varepsilon}_{QC}$ = 351 1/(M•cm)	
• Other properties from Table 1	
Case 2	The molar absorptivity of QC
	0, 100, and 351 1/(M•cm^1)
• 30 wt% MOST	
• 1 mm thickness	
• $\overline{\varepsilon}_{NBD}$ = 4590.8 1/(M•cm)	
• Other properties from Table 1	
Case 3	The energy density of MOST molecules
	0.1 MJ/kg, 0.22 MJ/kg, 0.3 MJ/kg, 0.44 MJ/
• 30 wt% MOST	kg, 0.6 MJ/kg, and 1 MJ/kg
• 1 mm thickness	
• $\overline{\varepsilon}_{NBD}$ = 4590.8 1/(M•cm) and	
$\overline{\varepsilon}_{QC}$ = 351 1/(M•cm)	
• Other properties from Table 1	
Case 4	The half-life time $t_{1/2}$
	1 h, 3 h, 6 h, 8 h, 10 h, 20 h
• 30 wt% MOST	$k = \ln(2)/(t_{1/2}$ (s))
• 1 mm thickness	
• $\overline{\varepsilon}_{NBD}$ = 4590.8 1/(M•cm) and	
$\overline{\varepsilon}_{QC}$ = 351 1/(M•cm)	
• Other properties from Table 1	

$$\overline{\varepsilon}_i = \frac{1}{\lambda_2 - \lambda_1} \int_{\lambda_1}^{\lambda_2} \varepsilon_i(\lambda) d\lambda \qquad (24)$$

where *i* stands for QC and NBD. For $[\lambda_1, \lambda_2]$ = [300 nm, 460 nm], the average molar absorptivities are $\overline{\varepsilon}_{NBD}$ = 4590.8 1/(M•cm) and $\overline{\varepsilon}_{QC}$ = 351 1/(M•cm).

For the following calculations we assume an illumination of the MOST film for 11 h, from 8.00 to 19:00, in the wavelength range between 300 nm and 460 nm, corresponding to the hourly solar irradiation flux depicted in Fig. 8b. The following 13 h are without irradiation. At noon, the maximum total solar irradiation is 1002.8 W/m^2. The average photon energy between 8:00 am and 18:00 pm, $\overline{E}_{300-460nm}$, is 4.91195 10^{-19} J, and the maximum irradiation in this wavelength range is 151.5 W/m^2 also occurring at 12:00 pm. Because this is the first time we present the model, we use the maximum solar irradiation to explore the extremes. However, the model is general and can be used to any solar irradiation flux for deeper analyses.

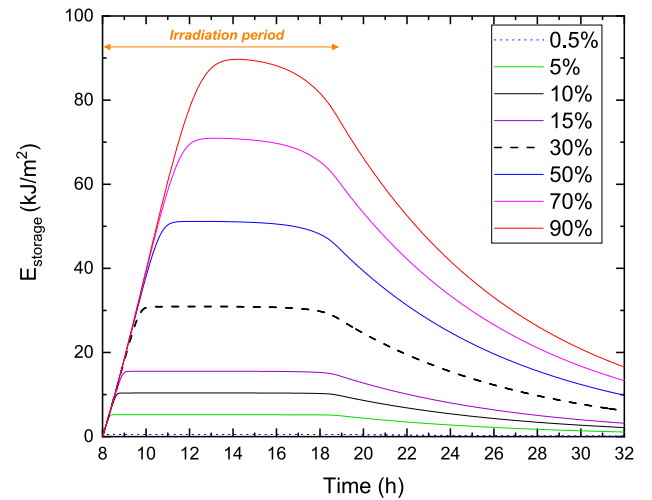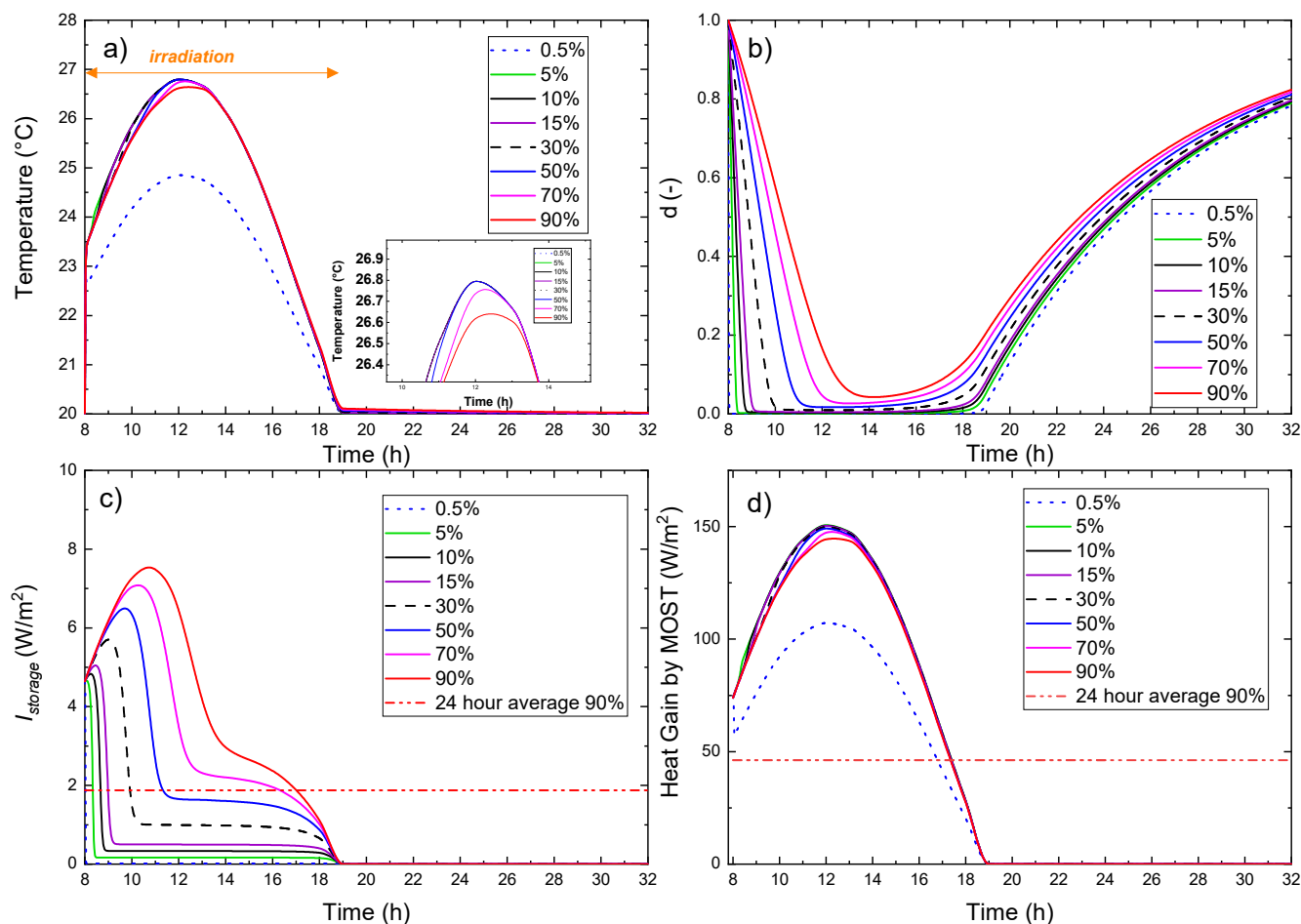Several parameters govern the performance of MOST films.

Fig. 9. The stored energy density in the MOST film for different concentrations of MOST molecules (wt. %), 1 mm thick film.

However, they can be classified in terms of functionality: storage time, energy density, and energy storage rate. These functionalities are covered with the following parametric study. The study concerns the effects of the MOST concentration in the matrix, the molar absorptivity of QC molecules, and the energy storage density of the NBD as well as the half-life time of the QC. The half-life time of the molecule that was newly designed for this work is relatively short (i.e., 1 h at room temperature) and does not fully fit to the day-night cycle that is of interest for window applications. Thus, a half-life time $t_{1/2}$, of 6 h will be used as default in the parametric studies. A thorough study of the effects of different half-life times for the heat release of the composite films is added. Table 2 summarizes all the case studies and input data in this section.

5.1.1. Case 1: Effects of MOST concentration

The increase in the MOST concentration or film thickness will automatically lead to the rise of the storage capacity of the MOST film. The stored energy (J/m^2) of the MOST film at each instant can be defined as follow:

$$E_{storage} = [QC] \bullet \Delta H_{storage} \bullet d \qquad (25)$$

The time scale in Fig. 9 starts at 8 h and ends 24 h later, at 32 h, when a new irradiation cycle may begin. Three distinct behaviors of the stored energy density can be seen in Fig. 9. At first, the stored energy density

Fig. 10. Effect of concentration of MOST system on the performance of the MOST film a) temperature evolution b) degree of transformation of NBD c) stored heat flux, d) heat gain by the MOST film (1 mm thick MOST film).

increases due to the photoisomerization of NBD to QC. The stored energy density then reaches a plateau or pseudo plateau due to the depletion of NBD and prevalence of QC in the film. After the irradiation period, the stored energy density decreases as a result of the back-conversion from QC to NBD, which is accompanied by a heat release.

In addition to the energy storage, there are various other processes that occur during the interaction of the MOST film with irradiation, such as heat gain by MOST film, irradiation transmission, and heat release. The thermal performance of the MOST film during and after the irradiation is exemplified by the following parameters: temperature of the film, chemically stored irradiation, and the heat gain by the MOST film (in the range 300–460 nm) (see Fig. 9). Many of the MOST film's properties depend on the state of conversion and the amount of NBD and QC in the film composite. To facilitate the comparison between the concentrations of NBD and QC, we define the degree of transformation of NBD as the ratio of the concentration of NBD molecules by the MOST molecules' initial concentration C_0:

$$\delta = \frac{[\text{NBD}]}{C_0} \tag{26}$$

δ takes values between 0 and 1, where 0 means all NBD are transformed into QC and vice versa.

The concentration of 0.5 wt% of the MOST molecules in the composite does not significantly affect the solar energy storage capabilities of the polystyrene composite (Fig. 9 and Fig. 10c). As it can be seen δ decreases sharply upon the irradiation and remains 0 until 18 h (Fig. 10b). Therefore, we investigated larger concentrations of MOST molecules in the polystyrene matrix, ranging from 0.5 wt% to 90 wt%.

The majority of NBD molecules are transformed to QC during the irradiation period as shown in Fig. 10b. Even in the case of highly concentrated film composite (90 wt%), 95 % of NBD molecules are converted to QC. However, the full back-conversion of QC molecules to NBD molecules is not reached before the new irradiation cycle (32 h).

For all the concentrations, the temperature of the MOST film (*in the middle of the film*) shows a bell shape curve (cf. Fig. 10a) similar to the evolution of the photon flux. The temperature of the film increases towards noon, reaching a maximum of 26.8 °C, due to the heat gain by MOST molecules (Fig. 10d). The MOST film with 0.5 wt% shows the lowest maximum temperature because at this concentration only 71 % of the irradiation is absorbed by the MOST film (cf. Appendix 2). Whereas for all other concentrations all incoming irradiation in the range 300 nm-460 nm is absorbed, meaning that the film is entirely opaque to wavelengths below 460 nm during the whole period of irradiation (cf. Appendix 2). Meanwhile, the maximum temperature of the film with 90 % wt. is lower than for the other concentrations (except for film with 0.5 wt% of MOST) (Fig. 10a, zoomed) as more solar energy is chemically stored compared to lower concentrations. The temperature increase of the MOST film can influence the rate constant of the back conversion k; the high temperature will lead to the acceleration of the back-conversion of QC molecules [20]. For small temperature changes, the impact on the back-conversion of QC might be neglected. However, for higher temperature change, this should be considered.

The irradiation is mainly absorbed as heat by the MOST film (Fig. 10d) regardless of MOST concentration, while only a small fraction is stored as chemical energy (Fig. 10c). The stored heat flux $I_{storage}$ is a dynamic property that depends on the irradiation conditions (cf. Eq.
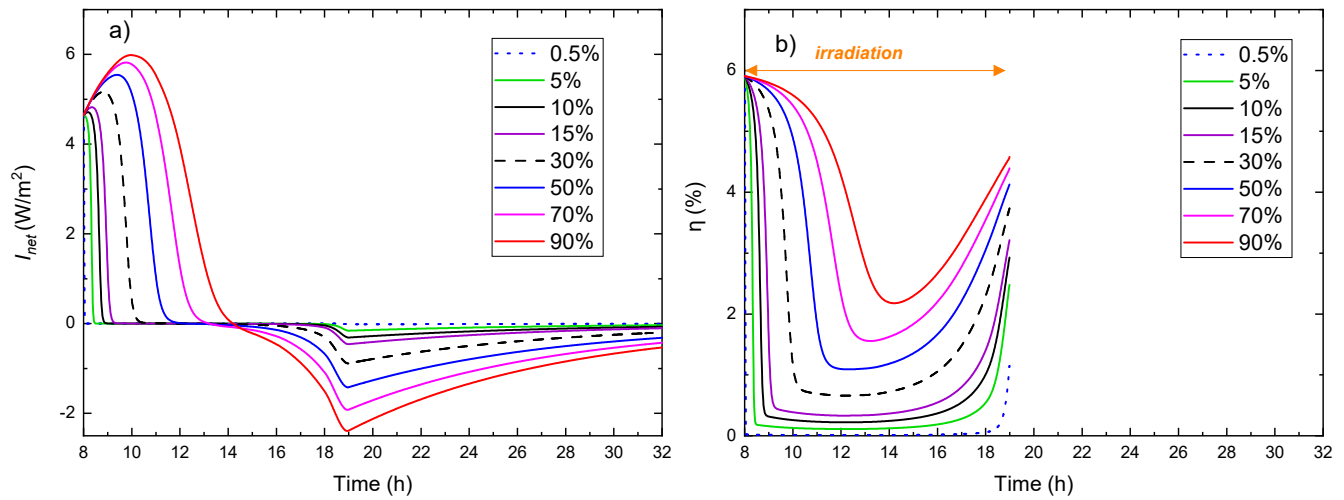
Fig. 11. Net stored heat flux and efficiency of the MOST film for different concentrations of MOST molecules in the composite.
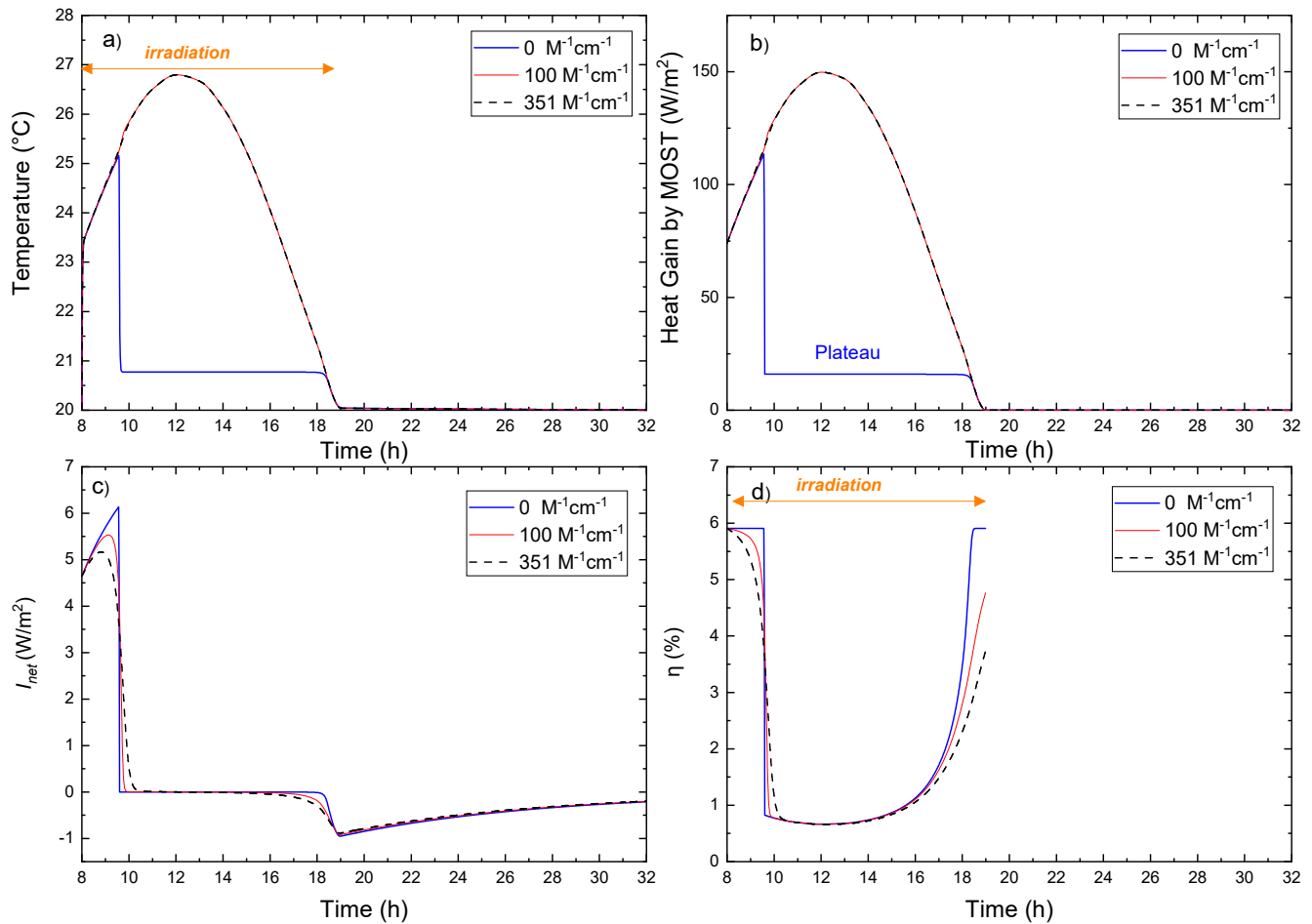

Fig. 12. Effect of molar absorptivity ($M^{-1} \cdot cm^{-1}$) of the MOST system on the performance of the MOST film a) Temperature, b) Heat gain by MOST, c) Net stored heat flux, and d) efficiency (1 mm thick MOST film and 30 wt% of MOST).

(13)), and the availability and characteristics of NBD molecules in the composite (wt%, ΔH_{iso} andϕ). However, the stored heat flux is not enough to describe the instantaneous state of storage. In fact, it does not consider the back-converted QC molecules and the associated heat release. To have an accurate and instantaneous indicator about the actually stored photons flux, we define the net stored heat flux I_{net}. As the difference between the stored photons flux and the heat released

from the MOST molecules in the composite:

$$I_{net} = I_{storage} - Q_{thermal\_iso} \bullet d \tag{27}$$

I_{net} is shown in Fig. 11a for the 24 h cycle. For up to 70 wt%, an idle period or zero heat balance can be observed between the stored flux (positive values) and the heat release flux (negative values). The latter
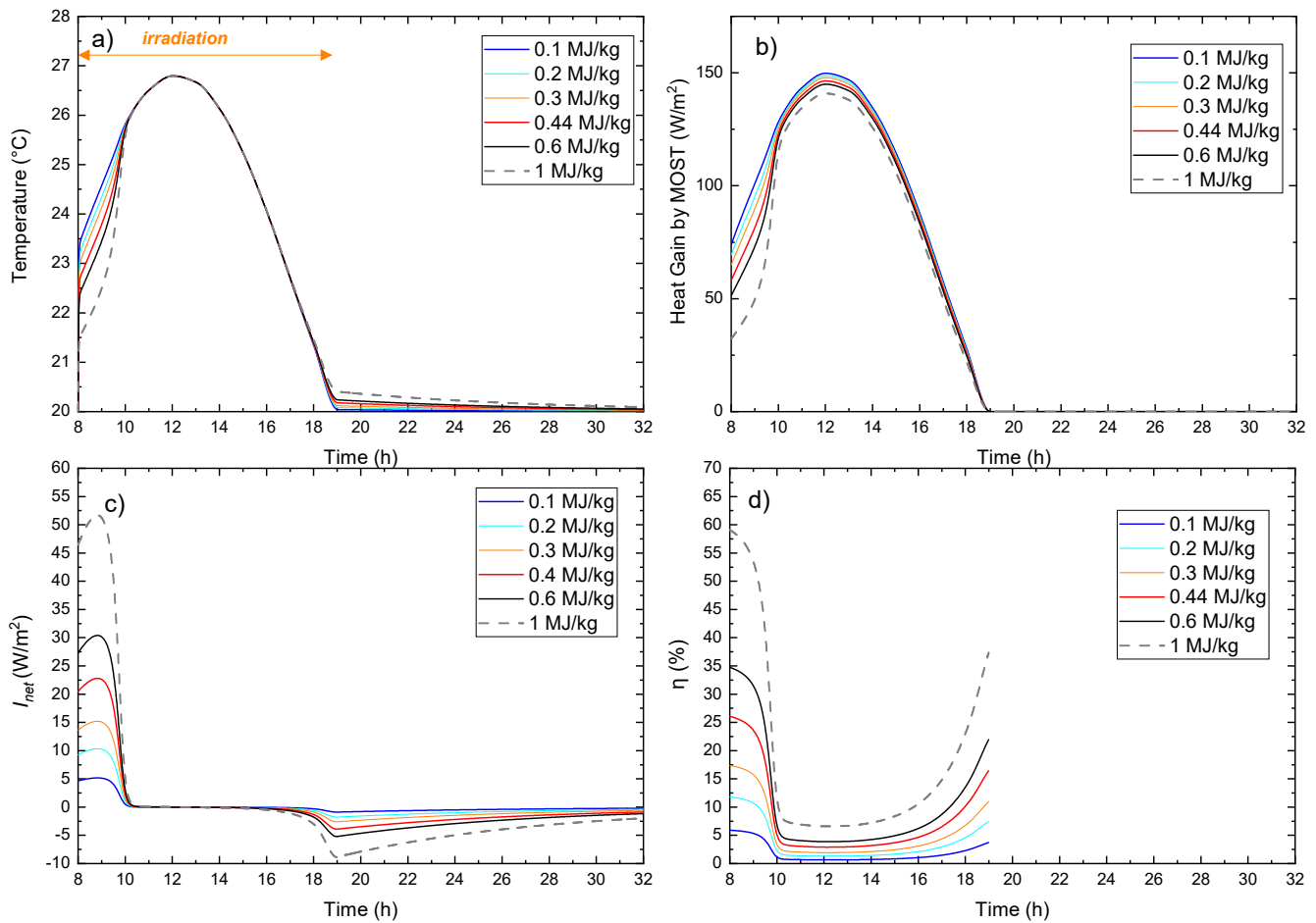
Fig. 13. Effects of the energy density of a MOST system on the performance of the MOST composite film a) Temperature, b) Heat gain by MOST, c) Net stored heat flux, and d) efficiency (1 mm thick MOST film containing 30 wt% of MOST molecules).

indicates the back-conversion of QC that takes place along with the irradiation (up to 19 h), and after the irradiation (after 19 h). For 90 % wt., the idle period does not exist; a positive balance of the I_{net} lasts up to about 14.2 h and then continues as a negative one. We can also see that the maximum net stored heat flux increases with increasing MOST concentration, reaching 6 W/m² for 90 wt% of MOST molecules. The heat release dominates after 14.2 h at the latest for all studied concentrations. The minimum of I_{net} for all concentrations occurs when the irradiation stops at 19 h, after that point in time only the back-conversion takes place.

Besides the net stored heat flux, another performance indicator is needed to characterize the performance of the MOST molecules regarding irradiation conditions and the available photons. Since the stored heat flux also includes the photon flux (cf. Eq. (12)), a division by the incoming irradiation will lead to an adimensional performance indicator. Thus, we define the instantaneous solar energy storage efficiency η as the ratio of the $I_{storage}$ over the incoming irradiation. η can be expressed in terms of MOST molecules properties as shown below:

$$\eta = 100 \bullet \frac{I_{storage}}{\dot{n} \bullet \overline{E}_{300-460nm}} \tag{28}$$

$$\eta = 100 \bullet \frac{\phi \bullet \beta_{NBD} \bullet \Delta H_{iso}}{\overline{E}_{300-460nm}} \tag{29}$$

The efficiency is defined over the irradiation period only, e.g. 19 h. The efficiency is proportional to the absorbed fraction of light by NBD molecules. Based on simulations, the maximum efficiency of 5.9 % of the film composite is obtained (cf. Fig. 11b) at the start of the irradiation (8

h) because the absorbed fraction of light by NBD is also at its maximum, $\beta_{NBD} = 1$. Thereafter, the storage efficiency decreases with the decrease in the concentration of NBD molecules. After 14 h, the efficiency starts to increase. This results from two simultaneous processes: the back-conversion of QC which provides more NBD molecules for solar energy storage, and the lower conversion rate from NBD to QC due to the reduction in the received photons flux (cf. Fig. 8b).

While it can be expected that η increases with the concentration of MOST molecules, the simulations reveal that the heat gain by the MOST is still dominating and represent most of the energy absorbed by the MOST film. This may not be the desired effect because the film releases sensible heat while it is irradiated. The heat gain results from the heat losses during the photoisomerization of NBD, and the photons absorbed by QC as thermal energy. The heat losses can be decreased by increasing the energy storage density and the QY of the MOST system, while the absorption of QC is governed by its molar absorptivity. To gain further understanding of the effects of QC absorption on the MOST film performance, we study in Case 2 the MOST film performance with a MOST concentration of 30 wt%, assuming different absorptivities for the QC molecules.

5.1.2. Case 2: Effects of molar absorptivity of QC

Although QC molecules do not participate in chemical energy storage in MOST film, they compete with NBD for available photons. If QC molecules would not absorb photons $\overline{\varepsilon}_{QC} = 0$ M⁻¹•cm⁻¹, the temperature of the MOST film would decrease instantaneously when all NBD molecules are converted to QC, as shown in Fig. 12a. Practically, it means that the MOST film becomes almost transparent to the irradiation
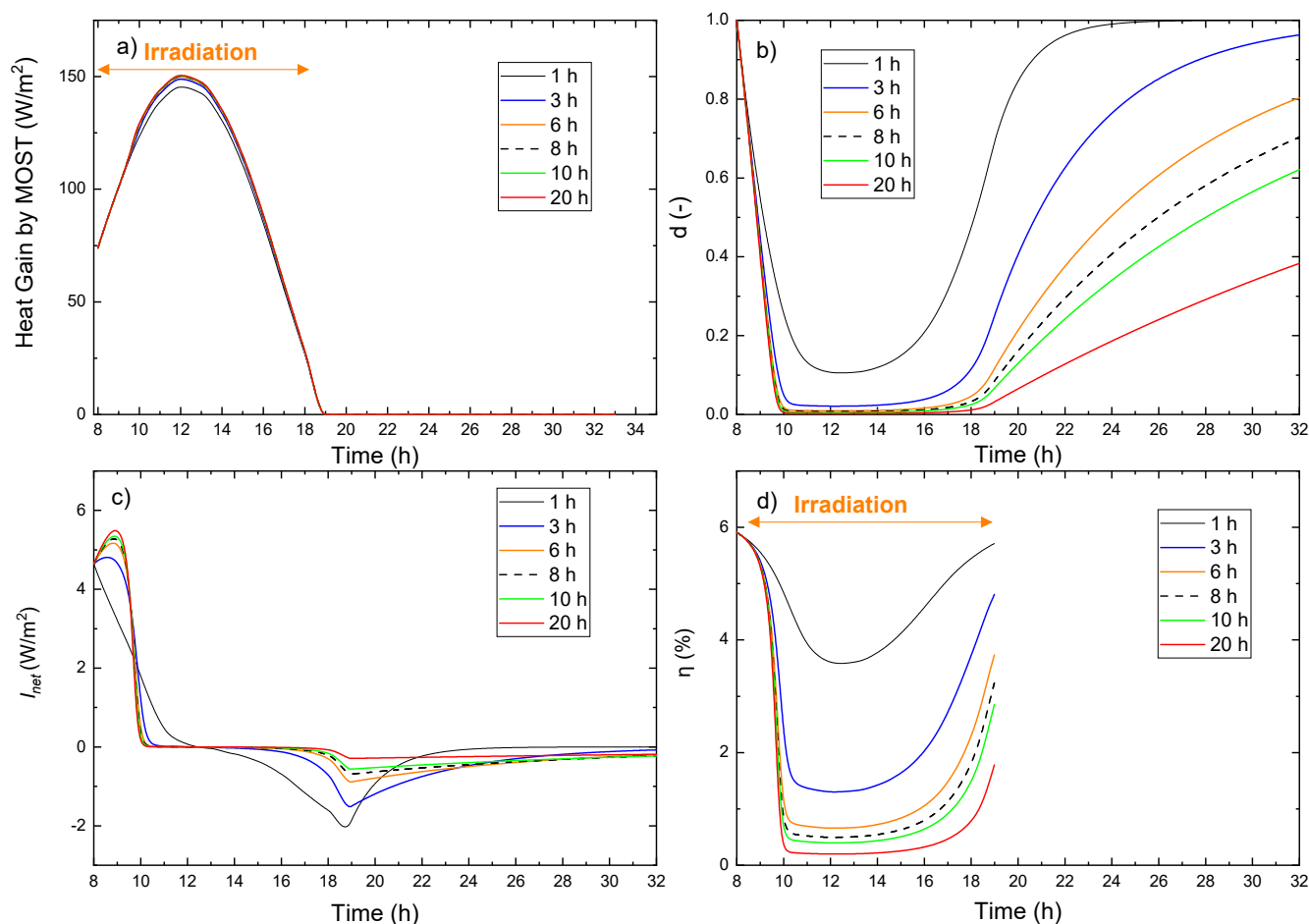
Fig. 14. Effects of half-life time of MOST system on the performance of the MOST film: 1 h, 3 h, 6 h, 8 h, 10 h, and 20 h (1 mm thick MOST film containing 30 wt% of MOST molecules).
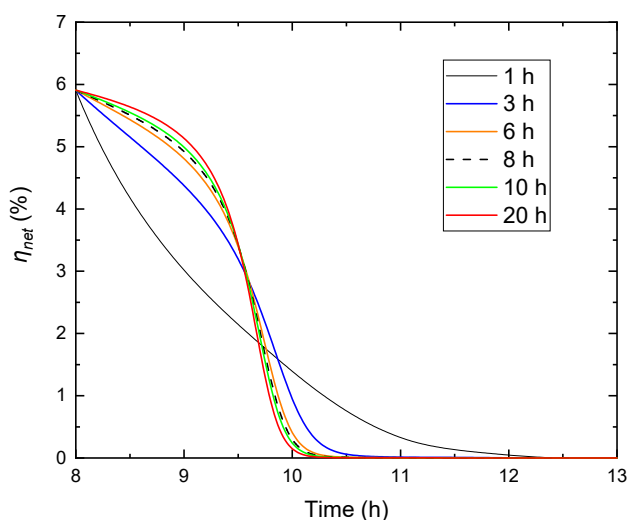

Fig. 15. The net efficiency for different half-life times.

Table 3
MOST and composite properties.

Molecule properties	Current molecule	Enhanced molecule
Quantum yield (%)	51.4	90
Energy density (kJ/mol)	34	150
Energy density (MJ/kg)	0.1	0.44
Molar absorptivity of QC (1/ (M•cm))	351	0
k (1/s)	$3.2\ 10^{-5}$ ($t_{1/2} = 6$ h)	$3.2\ 10^{-5}$ ($t_{1/2} = 6$ h)
wt. (%)	30	30
d (m)	0.001	0.001

in the range 300–460 nm. Consequently, the heat gain by the MOST system is also drastically decreased and levels off at a plateau, as shown in Fig. 12b. The plateau develops due to the back-conversion of QC to NBD. Thus, new NBD molecules (i.e., k•[QC]) are continuously present in the matrix for photoisomerization, leading to a constant heat gain due to photoisomerization heat losses.

We found that for $\bar{\varepsilon}_{QC} > 0$, the charging process of the MOST film (positive I_{net}) lasts longer but the stored flux I_{net} is overall smaller, as seen in c. Further we found that the distinct heat release of the back conversion (i.e., negative value) starts sooner. The latter observation is not trivial since the heat release from QC is not directly related to the absorption properties of the QC molecules. After the "complete" conversion of NBD molecules, there is continuously a small amount of NBD molecules present in the film due to the back-conversion of the QC molecules. Under the same irradiation conditions, the number of NBD molecules that have converted to QC molecules is higher for non-absorbing QC molecules ($\bar{\varepsilon}_{QC} = 0$) as compared to the absorbing QC ($\bar{\varepsilon}_{QC} > 0$). This in turn leads to higher energy storage and a higher I_{net} even after the complete conversion of NBD.

Thus, we conclude that the MOST system efficiency can be enhanced by designing a molecule which does not absorb in its QC form.
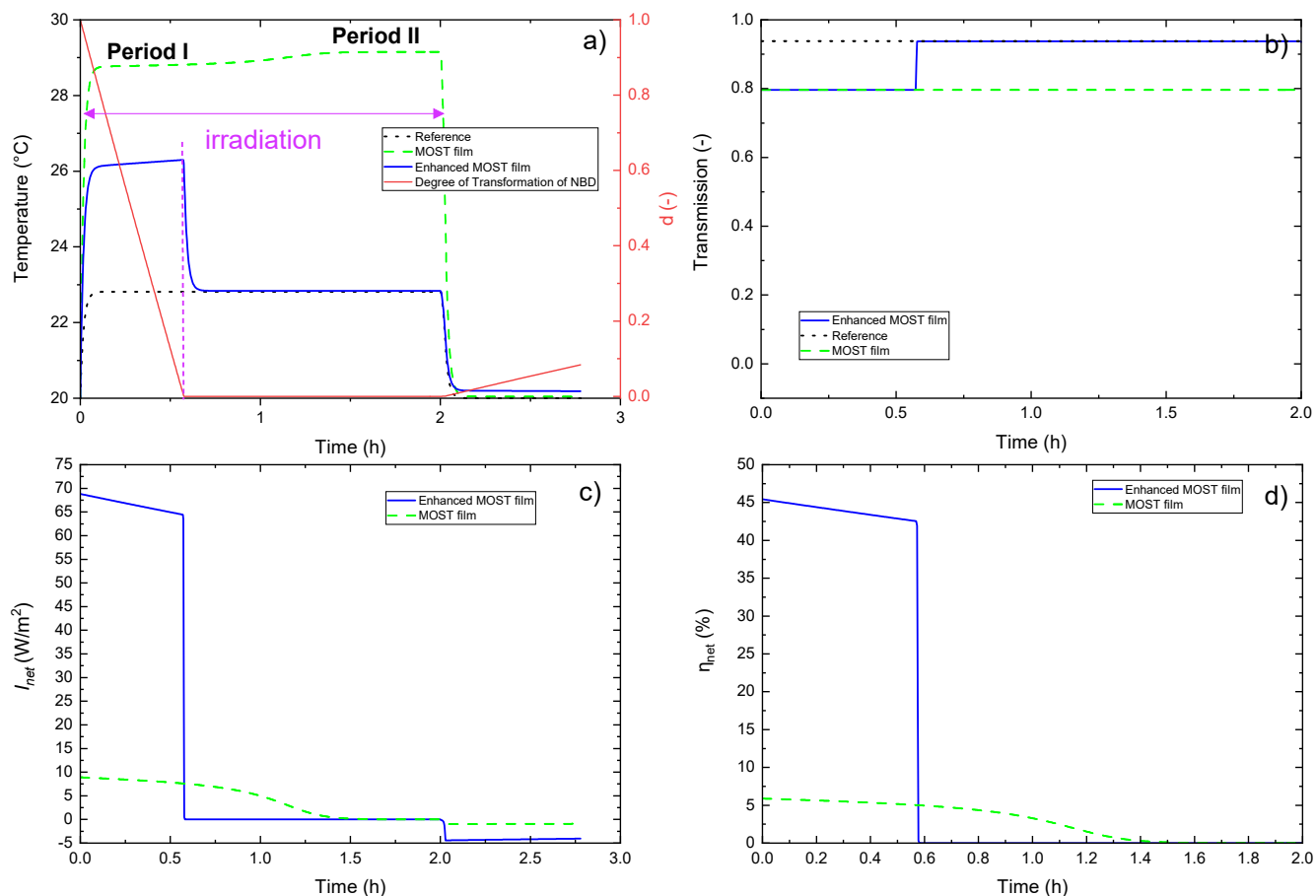
in the NBDs as chemical energy. Consequently, the heat gain of the film decreases with the increasing energy storage density of the MOST composite, as shown in Fig. 13b. The heat gain caused by the QC molecules is the same for all studied cases since it does not depend on the energy density. After the irradiation period (i.e., after 19 h), more heat is released from the high energy density molecules, and the temperature of the film is slightly higher (cf. Fig. 13a). Finally, both I_{net} and η are higher in the case of higher energy densities. For 0.1 MJ/kg and 1 MJ/kg, the net stored flux goes from 4.6 W/m^2 to 46.4 W/m^2, and the efficiency goes from 5.9 % to 59 %.

5.1.4. Case 4: Effect of half-life time

In all previously discussed model cases, all the molecules have the same half-life time of 6 h. As seen previously, the back-conversion is not complete within a 24 h cycle. The objective of this section is therefore to investigate different half-life times and their impact on the performance of the MOST film.

In the following we varied the rate constant k between $1.92\ 10^{-4}\ 1/s$ to $9.62\ 10^{-6}\ 1/s$, which corresponds to half-life times ranging from 1 h to 20 h (all other MOST film's parameters are unchanged as shown in Table 2). The results of the simulation presented in Fig. 14 show that the half-life time has a significant impact on the energy performance of the film. The heat gain of the film is the lowest for composites with MOST molecules that show the shortest half-life time (1 h) (Fig. 14a). This can be attributed to the fast back-conversion of the QC molecules to NBD molecules, which then in turn participate recurrently in the solar energy storage and thus reduce the amount of energy absorbed directly as heat. However, the fast back-conversion contributes to the heat gain of the film by releasing parts of the stored energy already during the illumination period.

The heat released during the night from the film containing MOST molecules with a half-life time of 1 h is comparably brief (cf. Fig. 14c) and the resulting heat flux reaches a maximum of 2 W/m^2. All the MOST molecules restore their NBD ground state during the night (cf. Fig. 14b). However, all of the studied films containing MOST molecules with half-life times longer than 1 h fail to regain their initial ground state overnight, e.g. only 96 % of QC molecules are back-converted to NBD over the course of 13 h for the MOST system with a half-life time of 3 h.

In the case of the film containing MOST molecules with a half-life time of 1 h, the instantaneous efficiency η maintains a higher value during the irradiation period (Fig. 14d). Since the back-converted QC molecules are participating recurrently in solar energy storage, they are increasing the storage capacity and the efficiency of the MOST film during daytime. However, the heat release due to the back-conversion increases the heat gain of the molecules and reduces the net amount of stored flux at each moment. Thus, we propose a new definition for the efficiency of MOST films, the net efficiency η_{net}, which is based on the net stored heat flux (Eq. (27)) instead of the stored heat flux:

$$\eta_{net} = 100 \bullet \frac{I_{storage} - Q_{thermal\_iso} \bullet d}{\dot{n} \bullet \overline{E}_{300-460nm}} \qquad (30)$$

The net efficiency of storage is by definition a positive quantity that is defined only over the irradiation period. The results for the net efficiency η_{net} in respect to different half-life times are shown in Fig. 15.

η_{net} decreases with irradiation time and lasts from 2 to 4 h, as shown in Fig. 15. When η_{net} drops to zero, the MOST system still stores solar irradiation. However, the heat release from QC starts dominating the net stored heat flux, as shown in Fig. 14c.

We conclude that the half-life time of the MOST molecules has a mayor influence on the efficiency of MOST films and on the generated heat release. For window applications, MOST systems with a half life-time between 3 and 6 h seem a good compromise between efficiency and peak power of the heat release, while also matching the time frame of the heat release with the heating demand after sunset.

5.2. Thermo-optical behavior of MOST film versus solar irradiation

So far, the MOST film's performance is studied only in the wavelength range of 300–460 nm. In this range, the polystyrene film absorbs only a small fraction of solar irradiation which can be neglected. However, over the rest of the solar spectrum, the polystyrene film absorbs solar irradiation and modifies the thermal behavior of the MOST film.

To evaluate the performance of a MOST film under the full solar spectrum, we simulated the performance of the composite film assuming solar irradiation from 300 nm to 2500 nm. The evaluation is done by direct comparison of MOST films and a polystyrene reference film (without MOST molecules). Two different MOST systems are considered. The ordinary NBD molecules studied earlier and an enhanced MOST system as shown in Table 3. The differences between the two MOST systems are in energy density, quantum yield, and molar absorptivity.

For the simulations we assume a solar irradiation corresponding to the irradiation at noon. First, solar irradiation is applied for two hours, followed by a recovery cycle. The two hours of irradiation were enough to reach a steady state in all the studied parameters, as shown in Fig. 16. The total solar irradiation at noon is 1002.8 W/m^2 (taken from data shown in Fig. 8). In the wavelength range 300 nm and 460 nm, the photon flux and energy are $3.07 \bullet 10^{20}$ photons/(m$^2 \bullet$s) and $4.93453 \bullet 10^{-19}$ J, respectively.

The three case studies showed different thermal and optical behavior versus solar irradiation, as shown in Fig. 16. We report in Fig. 16*a and b* the simulated temperature and transmitted solar irradiation of the MOST film and polystyrene film. The MOST film with the ordinary NBD/QC reaches a higher temperature than the reference film and the MOST film with the enhanced NBD/QC. The MOST film absorbs photons and gains heat through various processes during the photoisomerization of NBD molecules, by the absorbing QC molecules ($\overline{\varepsilon}_{QC} = 35.1\ 1/(M\bullet cm)$) and by the polystyrene matrix. The latter absorbs solar irradiation mainly in the wavelength's range 460–2500 nm. This leads to heat gain and film temperature rise, as shown in Fig. 16a. During the irradiation, the temperature profile of the MOST film can be divided into two behaviors: period I - during which the MOST system stores the photons' energy as chemical energy; period II - after the complete conversion of NBD, the irradiation is mainly converted to heat, resulting in an increase of the temperature of the film. During the whole period of irradiation, the MOST film transmits 80 % of the solar irradiation, while reference film transmits 94% (cf. Fig. 16b). However, in case of the enhanced MOST film (cf. degree of transformation in Fig. 16a), the temperature drops to a level that is almost the same as the temperature of the reference film once total conversion of the NBD molecules is reached. As a result, one can observe a sharp decrease in the heat gain of the film, in other words a higher transmission of the solar irradiation (cf. Fig. 16b).

The transparency of the enhanced MOST film switches from 80 % at the beginning of the irradiation process to 94% after the NBD molecules' complete conversion, providing a time/irradiation dependent optical and thermal behavior to the MOST film. The net efficiency of the enhanced MOST film reaches a maximum of 45% (Fig. 16*d*) after which the efficiency decreases sharply once the conversion of the NBD saturates.

Going back to the learnings from case 1 (cf. Fig. 11b), it becomes clear that the net efficiency of 45 % could be even further increased by increasing the concentration of MOST molecules in the film.

In summary, these results illustrate how drastic the differences in thermal and optical performance of MOST films system can be, depending on the design of the MOST molecule. With optimized molecular design it is possible to improve at the same time 1) the efficiency of the energy harvesting, 2) the magnitude and power of the heat release, as well as to reduce undesirable heat gain during illumination periods. This highlights the importance of detailed simulations that predict the behavior of MOST films in real life scenarios, in order to optimize the molecule design for specific applications.

5.3. Performance and potential of MOST composites for the design of energy efficient windows

In this work we studied the optical and energy performance of MOST composite films over a day and night cycle, with the goal of evaluating the potential of the material for the design of energy efficient windows. For an in-depth assessment of the potential of the material, further simulations would be necessary, taking into account other boundary conditions, different combinations of glass and MOST composite panes, as well as gas fillings and edge effects. However, the results obtained in this work allow a rough analysis of the potential of MOST materials for window applications as presented hereafter.

For the domestic sector, we assume a model house with ca. 100 m^2 habitable surface and a window surface of 30 m^2. To estimate the heat loss through a window, we assume a window with an insulation value (U-value) of 1 W/Km^2, which is representative for a contemporary energy-efficient window. For an autumn (winter) day with outdoor temperatures of 10 °C (0 °C) and an indoor temperature of 20 °C, the heat loss rate amounts to 10 W/m^2 (20 W/m^2). The total heat loss through all the windows of the model house is thus 300 W, equivalent to 7.2 kWh/day, in autumn and 600 W, or 14.4 kWh/day, on a winter day.

In comparison, the enhanced MOST composite film presented in Section 5.1 can store 1320 kJ/ m^2 (0.37 kWh/m^2) at full charge. Thus, the maximum amount of energy that could be stored in the window surfaces of our model house amounts to 11 kWh, which is in the same range as the total heat loss through the windows. The net heat flux of the heat release of the enhanced film reaches 4 W/m^2 in the hours just after sunset, equivalent to 40% of the heat loss rate in autumn and 20% of the heat loss rate in winter.

However, the simulation in 5.1 is based on the solar irradiation at noon on a sunny summer day with 1002.8 W/m^2. Further, the model house assumptions do not account for the orientation of the windows in space.

Thus, in a real application scenario, the upper limit of the energy that can be utilized with MOST materials is limited by the incident solar radiation in the absorption range on the respective day. To put the presented values into a context, we approximate that on a typical day in norther Europe, the sun provides about 1.6 kWh/m^2 in autumn 0.4 kWh/m^2 in winter. A panel that absorbs all UV irradiation, which corresponds to ca. 5% of the available solar energy, could thus harvest and store a maximum of 0.08 kWh/m^2 and 0.02 kWh/m^2 per autumn or winder day, respectively. In the case of our model house, this translates to an upper limit of ca. 2.4 kWh (0.6 kWh) of solar energy that could be utilized per autumn (winter) day. Thus, an optimized MOST system could contribute up to 5% of the daily energy required for heating on an autumn day, and 0.5% on a winter day.

This highlights, that the highest benefit of a MOST system is obtained on sunny and moderately cold days, such as spring or autumn days in Europe or North America or year-round in areas with continental climate. Further, would the impact of such MOST windows increase for highly insulated houses with low heating needs.

6. Conclusions

In this work, a new concept of solar energy storage in transparent films, using photo-switchable molecules (MOST), is investigated. The multi-physical modeling and simulations were conducted to evaluate the interaction of MOST films with light, studying their optical properties, as well as the dynamic energy storage. First, the performance of the MOST films were studied under the irradiation of the monochromatic light and validated for different concentrations of MOST molecules in the composite and different film thicknesses. Then, a complete model was developed, which describes the interaction of the MOST film with the entire spectrum solar irradiation. The findings can be summarized as follow:

- The MOST film of 1 mm thickness, containing 5 wt% or more of MOST molecules, absorbs 100 % of the solar irradiation in the wavelength range of 300 and 460 nm, making it an efficient UV shield.
- The studied molecule allows for a net stored flux of solar irradiation of 8.9 W/m^2, corresponding to the net storage of 8 Wh/m^2 per day, for a composite film containing 30 wt% of MOST molecules. However, the largest part of the absorbed photon flux/energy results in a heat gain. Thus, the temperature of MOST film increases by 9.1 °C, as compared to 2.8 °C for the polystyrene reference. In an application scenario in windows, this would prevent solar irradiation in the range of [300 nm, 460 nm], it prevents from entering the building, thus limit in the heat gain of the interior. At the same time, it also prevents the degradation of objects by UV irradiation.
- To compare different MOST molecules, the net efficiency of the system, η_{net}, was defined as a performance criterion including information about the stored heat flux, heat release, and photon flux. This criterion can be enhanced substantially by increasing ΔH_{iso}, QY and k. The current MOST molecule net efficiency is 5.9 % and can be increased further to at least 45% in the case of the enhanced MOST molecules, leading to a lower heat gain by the MOST film and a lower temperature change of the MOST film during the irradiation period.
- The maximum net efficiency lasts longer for the non-absorbing QC molecules. However, the MOST film becomes almost transparent to irradiation in the range of 300 and 460 nm after the complete conversion of NBD molecules. Therefore, a sharp time-dependent optical and thermal behavior (switch on/off) can be obtained by considering a non-absorbing QC molecule.

The parametric study showed the impact of each molecular and composite characteristic on the MOST film energy storage, losses, and optical behavior. The developed model is detailed and can be used to investigate pathways for the future development of MOST molecules for specific applications. The various parameters that can be varied in the MOST molecules offer a versatile molecule with entirely different behaviors, increasing potential applications. An optimization algorithm coupled with the developed model can tailor the MOST film characteristics to a specific application constraint (energy efficiency, transmittance, UV-protection, surface temperature, cooling needs, etc..)

However, the back-conversion of the molecules in the matrix needs to be further understood to accurately predict the concentration of NBD/QC over multiple cycles. On the same note, the aging and durability of the MOST film have to be thoroughly studied under solar irradiation for the designed molecules and the suitable polymer matrices.

CRediT authorship contribution statement

Zakariaa Refaa: Conceptualization, Methodology, Software, Formal analysis, Validation, Writing – original draft, Visualization, Writing – review & editing. **Anna Hofmann:** Conceptualization, Methodology, Investigation, Validation, Writing – review & editing. **Marcial Fernández Castro:** Investigation, Data curation. **Jessica Orrego Hernandez:** Investigation, Data curation, Formal analysis. **Helen Hölzel:** Conceptualization, Investigation, Data curation, Formal analysis. **Zhihang Wang:** Investigation, Data curation, Formal analysis. **Jens Wenzel Andreasen:** Funding acquisition, Writing – review & editing. **Kasper Moth-Poulsen:** Conceptualization, Project administration, Writing – review & editing, Supervision. **Angela Sasic Kalagasidis:** Conceptualization, Methodology, Funding acquisition, Project administration, Writing – review & editing, Supervision.

Declaration of Competing Interest

The authors declare that they have no known competing financial interests or personal relationships that could have appeared to influence the work reported in this paper.

Appendix 1. Spectral linear absorption coefficient

The film's transmission and absorption is calculated as follow:
With the spectral transmittance of PS film of thickness d: $\tau_\lambda = \exp(-\kappa_{\lambda PS} \bullet d)$

$$\alpha_\lambda + \tau_\lambda = 1$$

The spectral linear absorption coefficient is deduced from the absorbance (cf. Fig. 17) as follow:

$$\exp(-\kappa_{\lambda PS} \bullet d) = 10^{-Abs} = \tau_\lambda$$

$$\kappa_{\lambda PS} = \frac{Abs \bullet \ln(10)}{d}$$

$\kappa_{\lambda PS}$ includes the reflection part of irradiation, leading to a higher value of absorption. To calculate the real linear absorption coefficient, we need to calculate the spectral transmittance $\tau_{\lambda-in}$ of light which enters the medium ($I_{in} = I_0 (1-R_\lambda)$) and to exclude the reflection R_λ, cf Fig. 18):

$$\tau_{\lambda-in} = \frac{I}{I_{in}}$$

$$\tau_{\lambda-in} = \frac{I}{I_0} \bullet \frac{I_0}{I_{in}} = \tau_\lambda \bullet \frac{1}{1-R_\lambda}$$

and $\kappa_{\lambda PS-real} = -\frac{ln(T_{in\lambda})}{d}$

For seek of simplicity, we assumed the same reflection at all wavelengths, we could then deduce $\kappa_{\lambda PS-real}$ from the transmission profile. In the following, we consider an 8% reflection of light at the PS film surface.

$$\kappa_{\lambda PS-real} = \ln\left(\frac{\tau_\lambda}{(0.92)}\right)$$

In the case of 1 mm polystyrene film, 9.22 W/m^2 is absorbed by the film in the range of 300 nm and 460 nm from total solar irradiation of 1002.8 W/m^2. The absorbed fraction of light represents 6 % of available irradiation in the wavelength 300 nm and 460 nm (151.5 W/m^2).

Appendix 2. Absorbed fraction of light

The absorbed fraction of light depends on the state of concentration of NBD and QC. The absorbed fraction of light in the range of 300 and 460 nm (Fig. 8b) is given in Fig. 19. The absorbed fraction of light is shown versus time for MOST films with different concentrations (case study 1).
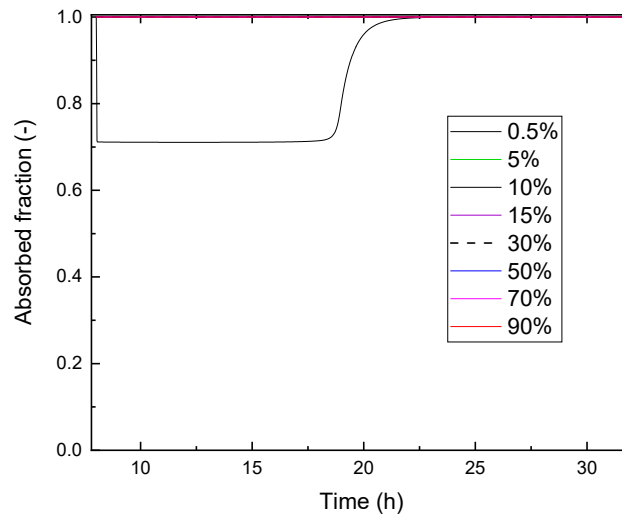

Fig. 19. Absorbed fraction of light for different MOST's concentrations (1 mm thick MOST film).

References

[1] European Commision. Mapping and analyses of the current and future (2020–2030) heating/cooling fuel deployment (fossil/renewables); 2020.

[2] Jelle BP. Solar radiation glazing factors for window panes, glass structures and electrochromic windows in buildings—Measurement and calculation. Sol Energy Mater Sol Cells 2013;116:291–323.

[3] Rezaei SD, Shannigrahi S, Ramakrishna S. A review of conventional, advanced, and smart glazing technologies and materials for improving indoor environment. Sol Energy Mater Sol Cells 2017;159:26–51. https://doi.org/10.1016/j. solmat.2016.08.026.

[4] Tällberg R, Jelle BP, Loonen R, Gao T, Hamdy M. Comparison of the energy saving potential of adaptive and controllable smart windows: a state-of-the-art review and simulation studies of thermochromic, photochromic and electrochromic technologies. Sol Energy Mater Sol Cells 2019;200:109828. https://doi.org/10.1016/j.solmat.2019.02.041.

[5] Aburas M, Soebarto V, Williamson T, Liang R, Ebendorff-Heidepriem H, Wu Y. Thermochromic smart window technologies for building application: a review. Appl Energy 2019;255:113522. https://doi.org/10.1016/j.apenergy.2019.113522.

[6] Casini M. Active dynamic windows for buildings: a review. Renew Energy 2018; 119:923–34. https://doi.org/10.1016/j.renene.2017.12.049.

[7] Jonsson A, Roos A. Evaluation of control strategies for different smart window combinations using computer simulations. Sol Energy 2010;84(1):1–9. https://doi.org/10.1016/j.solener.2009.10.021.

[8] Grynning S, Goia F, Time B. Dynamic thermal performance of a PCM window system: characterization using large scale measurements Steinar. Energy Procedia 2015;78:85–90. https://doi.org/10.1016/j.egypro.2015.11.119.

[9] Gao Y, Zheng Q, Jonsson JC, Lubner S, Curcija C, Fernandes L, et al. Parametric study of solid-solid translucent phase change materials in building windows. Appl Energy 2021;301:117467. https://doi.org/10.1016/j.apenergy.2021.117467.

[10] Orrego-Hernández J, Dreos A, Moth-Poulsen K. Engineering of norbornadiene/quadricyclane photoswitches for molecular solar thermal energy storage applications. Acc Chem Res 2020;53(8):1478–87. https://doi.org/10.1021/acs.accounts.0c00235.

[11] Pianowski ZL. Recent implementations of molecular photoswitches into smart materials and biological systems. Chem - A Eur J 2019;25(20):5128–44. https://doi.org/10.1002/chem.201805814.

[12] Sun C-L, Wang C, Boulatov R. Applications of photoswitches in the storage of solar energy. ChemPhotoChem 2019;3(6):268–83. https://doi.org/10.1002/cptc.201900030.

[13] Miki S, Asako Y, Yoshida Z-I. Photochromic solid films prepared by doping with donor-acceptor norbornadienes. Chem Lett 1987;16(1):195–8. https://doi.org/10.1246/cl.1987.195.

[14] Mansø M, Petersen AU, Wang Z, Erhart P, Nielsen MB, Moth-Poulsen K. Molecular solar thermal energy storage in photoswitch oligomers increases energy densities and storage times. Nat Commun 2018;9(1). https://doi.org/10.1038/s41467-018-04230-8.

[15] Petersen AU, Hofmann AI, Fillols M, Mansø M, Jevric M, Wang Z, et al. Solar energy storage by molecular norbornadiene-quadricyclane photoswitches: polymer film devices. Adv Sci 2019;6(12):1900367. https://doi.org/10.1002/advs.v6.1210.1002/advs.201900367.

[16] Huang Y, El Mankibi M, Cantin R, Coillot M. Application of fluids and promising materials as advanced inter-pane media in multi-glazing windows for thermal and energy performance improvement: a review. Energy Build 2021;253:111458. https://doi.org/10.1016/j.enbuild.2021.111458.

[17] Mony J, Climent C, Petersen AU, Moth-Poulsen K, Feist J, Börjesson K. Photoisomerization efficiency of a solar thermal fuel in the strong coupling regime. Adv Funct Mater 2021;31(21):2010737. https://doi.org/10.1002/adfm.v31.2110.1002/adfm.202010737.

[18] Wardle B. Principles and Applications of Photochemistry, vol. 36. John Wiley & Sons, Ltd; 2009. https://doi.org/10.1080/09500348914551321.

[19] Gauglitz G. Photophysical, photochemical and photokinetic properties of photochromic systems. photochromism, vol. 1. Elsevier; 2003, p. 15–63. https://doi.org/10.1016/B978-044451322-9/50006-3.

[20] Stranius K, Börjesson K. Determining the photoisomerization quantum yield of photoswitchable molecules in solution and in the solid state. Sci Rep 2017;7:1–9. https://doi.org/10.1038/srep41145.

[21] Dreos A, Börjesson K, Wang Z, Roffey A, Norwood Z, Kushnir D, et al. Exploring the potential of a hybrid device combining solar water heating and molecular solar thermal energy storage. Energy Environ Sci 2017;10(3):728–34.

[22] American Society of Heating, Refrigerating and Air-Conditioning Engineers I. ASHRAE Handbook – Fundamentals. American Society of Heating, Refrigerating and Air-Conditioning Engineers, Inc. (ASHRAE); 2017.

[23] Hagentoft C-E. Introduction to building physics. Studentlitteratur AB; 2001.

[24] Quant M, Hamrin A, Lennartson A, Erhart P, Moth-Poulsen K. Solvent effects on the absorption profile, kinetic stability, and photoisomerization process of the norbornadiene-quadricyclanes system. J Phys Chem C 2019;123:7081–7. https://doi.org/10.1021/acs.jpcc.9b02111.